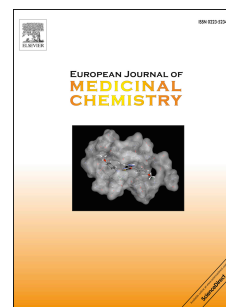# Journal Pre-proof

Development of chalcone-*O*-alkylamine derivatives as multifunctional agents against Alzheimer's disease

Ping Bai, Keren Wang, Pengfei Zhang, Jian Shi, Xinfeng Cheng, Qi Zhang, Cheng Zheng, Yao Cheng, Jian Yang, Xiaoxia Lu, Zhipei Sang

Please cite this article as: P. Bai, K. Wang, P. Zhang, J. Shi, X. Cheng, Q. Zhang, C. Zheng, Y. Cheng, J. Yang, X. Lu, Z. Sang, Development of chalcone-*O*-alkylamine derivatives as multifunctional agents against Alzheimer's disease, *European Journal of Medicinal Chemistry* (2019), doi: https://doi.org/10.1016/j.ejmech.2019.111737.

This is a PDF file of an article that has undergone enhancements after acceptance, such as the addition of a cover page and metadata, and formatting for readability, but it is not yet the definitive version of record. This version will undergo additional copyediting, typesetting and review before it is published in its final form, but we are providing this version to give early visibility of the article. Please note that, during the production process, errors may be discovered which could affect the content, and all legal disclaimers that apply to the journal pertain.
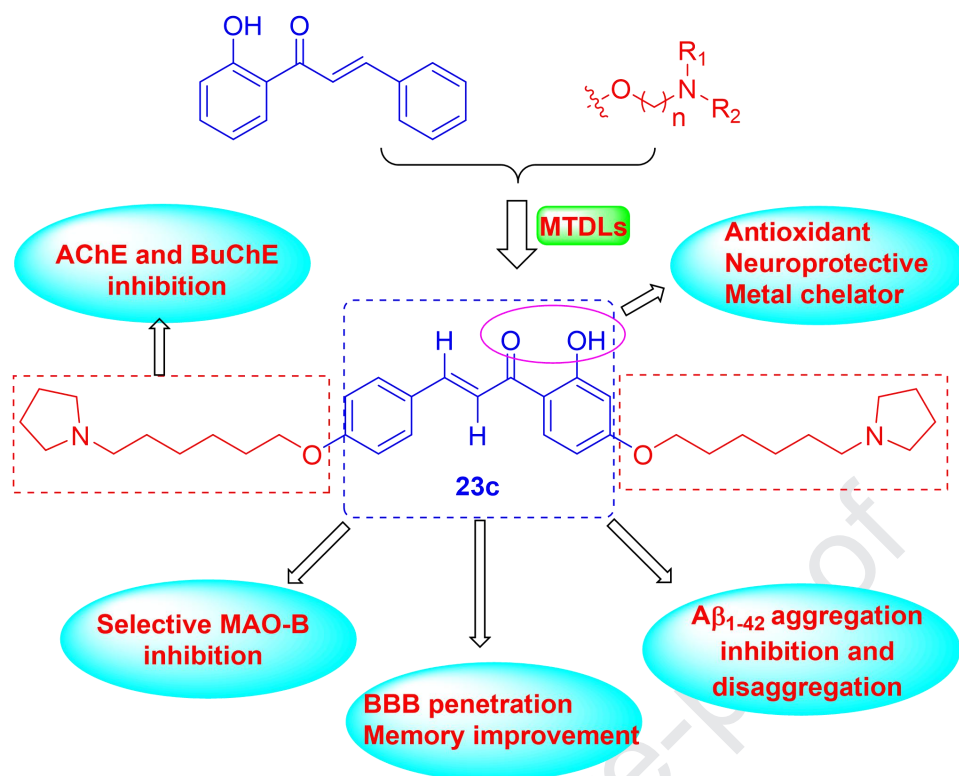
Development of chalcone-*O*-alkylamine derivatives as multifunctional agents against Alzheimer's disease

Ping Bai[a,d, #], Keren Wang [b,#], Pengfei Zhang[c,#], Jian Shi[b], Xinfeng Cheng[b], Qi Zhang[a], Cheng Zheng[a], Yao Cheng[a], Jian Yang[a], Xiaoxia Lu[a, *] Zhipei Sang[b, *]

[a] Chengdu Institute of Biology, Chinese Academy of Sciences, Chengdu 610041, PR China

[b] College of Chemistry and Pharmaceutical Engineering, Nanyang Normal University, Nanyang, 473061, PR China

[c] School of Medicine, Henan University Minsheng College, Kaifeng, 475000, PR China

[d] University of Chinese Academy of Sciences, Beijing 100049, PR China

*Corresponding authors.

E-mail: luxx@cib.ac.cn (Xiaoxia Lu)

E-mail: sangzhipei@126.com (Zhipei Sang)

#These authors contributed equally.

Abstract

A series of novel chalcone-*O*-alkylamine derivatives were designed, synthesized and evaluated as multifunctional anti-Alzheimer's disease agents. Based on the experimental results, compound **23c** exhibited good inhibitory potency on both acetylcholinesterase ($IC_{50} = 1.3 \pm 0.01$ μM) and butyrylcholinesterase ($IC_{50} = 1.2 \pm 0.09$ μM). Besides, **23c** exhibited selective MAO-B inhibitory activity with IC_{50} value of 0.57 ± 0.01 μM. Compound **23c** was also a potential antioxidant and neuroprotectant. In addition, compound **23c** could inhibit self-induced $A\beta_{1\text{-}42}$ aggregation. Moreover, compound **23c** was a selective metal chelator, and could inhibit and disaggregate Cu^{2+}-induced $A\beta_{1\text{-}42}$ aggregation, which was supported by the further transmission electron microscopy images. Furthermore, **23c** could cross the blood-brain barrier *in vitro*, and improved scopolamine-induced memory impairment *in vivo* assay. Molecular modeling studies showed that **23c** could bind to the active site of AChE, BuChE, $A\beta_{1\text{-}42}$ and MAO-B. Taken together, these results suggested that compound **23c** might be a potential multifunctional agent for the treatment of AD.

Keywords: Alzheimer's disease; Chalcone-*O*-alkylamine derivatives; Multi-functional agents; Rational design; Synthesis; Precognitive effect.

Abbreviations: AD, Alzheimer's disease; NMDA, *N*-methyl-D-aspartate receptor; ACh, acetylcholine; AChE, acetylcholinesterase; BuChE, Butyrylcholinesterase; Aβ, β-amyloid; APP, amyloid precursor protein; MAO-B, monoamine oxidase B; MAO-A, monoamine oxidase A; FAD, flavin adenine dinucleotide; PD, Parkinson disease; FDA, Food and Drug Administration; MTDLs, multi-target-directed ligands; ORAC-FL, Oxygen Radical Absorbance Capacity; ThT, thioflavin T; PDB, protein data bank; BBB, blood-brain barrier; CNS, central nervous system; TEM, transmission electron microscopy; MTT, 3-(4,5-dimethylthiazol-2-yl)-2,5- diphenyltetrazolium; PAMPA, parallel artificial membrane permeation.

1. Introduction

Alzheimer's disease (AD) is characterized by deterioration of memory, decline in language skills, and other cognitive impairments in elder people [1]. To date, more than 46.8 million people worldwide are diagnosed with AD and this number will continue to increase. With the increasing of its incidence, AD has caused a huge economic impact on both individuals and society [2]. Currently, despite enormous efforts made in the discovery of anti-AD drugs, there are only three acetylcholinesterase inhibitors (donepezil, rivastigmine and galantamine) and one *N*-methyl-D-aspartate receptor (NMDA) antagonist (memantine) that are approved for AD treatment. Though those drugs can relieve some symptoms of AD patients, they are not able to reverse the disease fundamentally [3, 4].

The pathogenic mechanism of AD is highly complicated, the exact etiology remains unknown. In recent years, with the continuous research on the neurochemical, physiological and pharmacological, the pathogenesis of AD has made progress [5]. Several hypotheses, such as cholinergic hypothesis [6], amyloid hypothesis [7], have been proposed to explain the mechanism of AD pathogenesis. The cholinergic hypothesis suggests that low level of acetylcholine (ACh) is the main cause of memory and cognitive impairment in AD patients. Accumulation of studies suggests that the acetylcholinesterase (AChE) plays an important role in the regulation of several physiological reactions by hydrolyzing the neurotransmitter ACh in cholinegic synapses [8]. Butyrylcholinesterase (BuChE) is an enzyme closely related to AChE and serves as a co-regulator of cholinergic neurotransmission by hydrolyzing ACh. In addition, with the progress of AD, the level of AChE in the brain decreases progressively, but BuChE activity remains the same or increases up to 165% of the normal level. In the advanced stage, BuChE takes over the hydrolysis of ACh in the AChE deficient brain. Specific BuChE inhibition results in a 5-fold increase in ACh levels and could circumvent the classical cholinergic toxicity that is a common side effect of AChE inhibition [9, 10]. Therefore, dual-inhibition of AChE and BuChE may be a better therapeutic strategy in the treatment of AD.

The "amyloid hypothesis" suggests that the β-amyloid (Aβ) plaques in the brain play a pivotal role in AD pathogenesis. The amyloid precursor protein (APP) is hydrolyzed by secretase enzymes to produce Aβ peptides that can aggregate into monomers, oligomers and Aβ plaques which can trigger the pathogenic cascade and finally cause the neuronal loss and dementia [7]. A$\beta_{1\text{-}40}$ and A$\beta_{1\text{-}42}$ are two key types of Aβ isoforms, A$\beta_{1\text{-}40}$ is present in larger amounts in the AD brain, yet A$\beta_{1\text{-}42}$ is more dissolutive and more prone to aggregate into fibrils and is more neurtoxic than A$\beta_{1\text{-}40}$ [11]. Additionally, excessive biometals including Cu^{2+}, Fe^{2+}, Zn^{2+} and Al^{3+} are found in the AD brains. These excessive biometals are known to interact with Aβ peptides and promote their aggregation [12]. Therefore, preventing the aggregation of A$\beta_{1\text{-}42}$ may provide a potent therapeutic strategy for AD treatment.

Oxidative stress also plays a crucial role in the development of AD [13]. Oxidative stress is often abnormal in the early stage of AD, and it is involved in the occurrence and development of AD. In the brains of the elder people, oxidized substances including nucleic acids, proteins, lipids and carbohydrates, cannot be eliminated, which lead to excessive oxidation of neuron cells [14]. Furthermore, oxidative stress can promote Aβ aggregation and further form neurofibrillary tangels [15]. Therefore, antioxidant agents could be an effective strategy for the treatment of AD.

Monoamine oxidases A and B (MAO-A and MAO-B) are important flavin adenine dinucleotide (FAD)-dependent enzymes that catalyze the oxidative deamination of monoamines [16]. MAO inhibitors have been proved to possess therapeutic effects on CNS-related diseases including depression, Parkinson disease (PD), AD, and so on [17]. Studies have shown that selective MAO-B inhibitors contribute to improve learning and memory [18]. Therefore, selective MAO-B inhibition is also deemed as a potential approach to treat AD.

So far, the drugs approved by the Food and Drug Administration (FDA) for clinical treatment of AD can only hit single target and have limited effects on mitigate or halt the progression of AD. In view of the multiple pathogenesis of AD, drugs which can simultaneously hit multiple targets could be a better strategy for AD treatment. Therefore, the multi-target-directed

ligands (MTDLs) strategy has been considered as an effective way for the treatment of AD, and some multifunctional agents have been developed and are in clinic trails [19-22]. These candidates, which could hit two or more AD-related targets, may represent a clinic advantage in the future.

Chalcones (1,3-diphenyl-2-propen-1-ones) (**Fig. 1**) are prominent secondary-metabolite precursors of flavonoids and isoflavonoids in plants. Chalcones and their derivatives have been well studied for drug design because of the multiple pharmacological activities (such as radical-scavenging, anti-tumor, anti-inflammatory, and neuroprotective properties) [23, 24]. Recent studies have shown that chalcones and their synthetic analogs exhibit potential bioactivities associated with neurological diseases especially for AD. For example, Choi, J. W. *et al*. reported that compounds with a chalcone scaffold exert MAO inhibitory activities for the treatment of AD [25]. One ^{18}F-radiolabeled chalcone analog is used as an Aβ imaging agent [26]. However, the lack of ChEs inhibition and metal chelation limited its application in AD therapy. Therefore, design and synthesis of novel chalcone derivatives based on the MTDLs strategy will increase pharmacological activities for the development of anti-AD drugs.

<Insert **Fig. 1**>

In our previous work, a series of genistein-*O*-alkylamines and scutellarin-*O*-alkylamine derivatives was designed and synthesized. Results showed that the *O*-alkylamine pharmacophore played the key role in cholinesterase inhibition [27, 28]. Moreover, it is reported that numerous anti-AD compounds with two symmetrical pharmacophoric units can exert a significantly higher ChE inhibitory potency [29-31]. Therefore, the *O*-alkylamine fragment is introduced into both aromatic rings of chalcone to obtain a series of novel chalcone-*O*-alkylamine derivatives (**Fig. 2**), in the hope of acquiring novel molecules possessing various multifunctional activities.

Based on the MTDLs strategy, a series of chalcone-*O*-alkylamine derivatives was designed and synthesized. The biological activities of these novel compounds were tested *in vitro* including AChE and BuChE inhibition, MAOs inhibition, effect on Aβ_{1-42} aggregation, antioxidant activity, biometals chelation, neuroprotective effect, the ability of cross blood-brain barrier (BBB)

in vitro and precognitive effect *in vivo*. Besides, docking studies were also performed to provide rational explanation for their biological activities.

<div align="center"><Insert Fig. 2></div>

2. Result and discussion

2.1. Chemistry

The synthetic route of the chalcone-*O*-alkylamine derivatives was indicated in **Scheme 1** and **Scheme 2**. Due to the presence of intramolecular hydrogen bonding, the 4'-OH of 2', 4'-dihydroxyacetophenone was more reactive than that of the 2'-OH, compounds **3-6** were easily synthesized from 2', 4'-dihydroxyacetophenone by using dibromo alkane in the presence of K_2CO_3 in anhydrous acetone under refluxing. Subsequently, **3-6** were reacted with corresponding secondary amines **a-d** and anhydrous K_2CO_3 in CH_3CN at 65 °C to obtain compounds **7-10**. Under the same condition, *p*-hydroxybenzaldehyde **11** was used as raw material to obtain compounds **16-19**. Finally, the target compounds **20-23** were prepared by condensation of the appropriate acetophenones **7-10** with the appropriate aldehydes **16-19** in ethanolic KOH solution. In addition, compounds **26a** and **26b** were obtained by the condensation of **24** with **10c** and **25** with **19c**, respectively. All new compounds were confirmed by ^{1}H NMR and HR-ESIMS, and parts of them were further characterized by ^{13}C NMR.

<div align="center"><Insert Scheme 1></div>

<div align="center"><Insert Scheme 2></div>

2.2. Pharmacology

2.2.1. Inhibition of AChE and BuChE.
The modified Ellman's method was used to evaluate AChE and BuChE inhibitory activities of target compounds [27]. AChE was from *electrophorus electricus*, and BuChE was from *equine serum*. Donepezil was used as a reference compound.

As shown in **Table 1**, most of the target compounds displayed moderate to good inhibitory activity against AChE and BuChE without obvious selectivity, showing that the introduction of *O*-alkylamines could significantly increase ChEs inhibitory capacity, which was consistent with our design strategy. According to the screening data in **Table 1**, both the length of the methylene chain and the structure of terminal groups NR_1R_2 of side chain significantly affected the

AChE/BuChE inhibitory activities. For AChE inhibition, the AChE inhibitory activity gradually increased as the methylene extended, and the optimal methylene was 6, such as **20a** (n = 2) > **21a** (n = 3) > **22a** (n = 4) > **23a** (n =6); **20b** (n = 2) > **21b** (n = 3) > **22b** (n = 4) = **23b** (n =6); **20c** (n = 2) > **21c** (n = 3) < **22c** (n = 4) > **23c** (n =6). In most conditions, when the length of the methylene chain remained the same, the potency to inhibit AChE was in the order: pyrrole > diethylamine > piperidine > benzylpiperidine, such as **20c** < **20d** < **20b** < **20a**; and **21c** < **21d** < **21b** < **21a**. Among these compounds, compound **21c** showed the best AChE inhibitory activity with IC_{50} value of 0.79 μM. For BuChE inhibition, when the terminal groups NR_1R_2 were benzylpiperidine, piperidine and pyrrole, the BuChE inhibitory activity increased as methylene chain extended, such as **20a** > **21a** > **22a** > **23a**, **20b** > **21b** > **22b** > **23b**, and **20c** > **21c** < **22c** > **23c.** When the methylene chain was 6, the tendency to inhibit BuChE was in the order: benzylpiperidine > pyrrole > piperidine > diethylamine, such as **23a** < **23c** < **23b** < **23d**. Particularly, compound **23a** showed the best BuChE inhibitory activity with IC_{50} value of 0.8 μM.

According to the above results, compound **23c** presented the balanced and high-efficiency dual AChE/BuChE inhibitory activity with IC_{50} values of 1.3 μM and 1.2 μM, respectively. In order to further evaluate the structure-activity relationship (SAR) of compound **23c**, compounds **26a** and **26b** were synthesized and tested the AChE/BChE inhibitory activity. As shown in Table 1, compound **26a** showed good AChE inhibitory activity with IC_{50} value of 4.2 μM and moderate BuChE inhibitory potency with IC_{50} value of 12.3 μM, and compound **26b** inhibited AChE/BuChE inhibitory activities with IC_{50} values of 8.9 μM and 50.2 μM, respectively, implying that compounds **26a** and **26b** were selective AChE inhibitors. In addition, compounds **26a** and **26b** exhibited lower ChEs inhibitory activity than compound **23c**, indicating that the symmetrical *O*-alkylamine fragment could contribute to AChE/BuChE inhibitory activity, which was consist with our design strategy. Further, compounds **23c**, **26a** and donepezil were investigated using *hu*AChE and *hu*BuChE, the results in **Table 2** showed that compound **23c** displayed good *hu*AChE and *hu*BuChE inhibitory activity with IC_{50} values of 0.78 μM and

0.91μM, respectively, and compound **26a** showed good *hu*AChE inhibitory activity with IC$_{50}$ value of 3.2 μM, implying that AChE inhibitory activity using human AChE was better than that using *ee*AChE.

<Insert **Table 1**>

<Insert **Table 2**>

2.2.2. Inhibition of human MAOs. The inhibitory activities toward MAO-A and MAO-B (recombinant human enzyme) were evaluated to further investigate the multi-potent biological profiles of the chalcone-*O*-alkylamine derivatives [32]. Iproniazid and rasagiline were also tested as referenced compounds. As shown in **Table 1**, most target compounds showed good MAO-B inhibitory activities with weak MAO-A inhibitory activities, indicating that the target compounds were selective MAO-B inhibitors, which contributed to AD treatment. In general, both methylene chain and terminal groups NR$_1$R$_2$ significantly influenced MAO-B inhibitory activity. When the NR$_1$R$_2$ was fixed, the MAO-B inhibitory activity increased as methylene chain extended, such as **20a** > **21a** > **22a** > **23a**, **20b** > **21b** > **22b** < **23b**, **20c** = **21c** > **22c** < **23c**, **20d** > **21d** > **22d** < **23d**. Moreover, when the methylene chain was determined, the compounds with cyclic amines (pyrrole and piperidine) showed better MAO-B inhibitory activity than compounds with benzylpiperidine. Especially, compound **23c** showed the best MAO-B inhibitory activity with IC$_{50}$ value of 0.57 μM. Further, the mono-substituted *O*-alkylamine derivatives **26a** and **26b** showed lower MAO-B inhibitory activity than disubstituted *O*-alkylamine derivative **23c**, implying that the disubstituted *O*-alkylamine fragment contributed to MAO-B inhibitory activity. Therefore, the results revealed that compound **23c** was a potent selective MAO-B inhibitor and presented good AChE and BuChE inhibitory activities, which was selected to perform further study.

2.2.3. Antioxidant activity in vitro. Next, we evaluated the antioxidant activity of the synthetic compounds using the ORAC-FL (Oxygen Radical Absorbance Capacity by Fluorescein) assay [27, 28]. As show in **Table 3**, most of the synthetic compounds exhibited good antioxidant activities *in vitro* with ORAC values of 0.96-1.4 Trolox (a synthetic analog of vitamin E) equivalents. The structure-activity relationship analysis indicated that the different substituent moiety NR$_1$R$_2$ and the length of methylene chain did not significantly affect the antioxidant activity. Compound **23c** showed good antioxidant activity with an ORAC value of 1.3 eq.

2.2.4. Inhibition of the self-mediated Aβ$_{1-42}$ aggregation. To gain further insight into the self-induced Aβ$_{1-42}$ aggregation inhibitory activity of synthetic chalcone-*O*-alkylamines derivatives,

the Thioflavin T (ThT) fluorescence method was used, and curcumin was also tested as the reference compound [27]. The results listed in **Table 3** indicated that most of the tested compounds showed good potencies (51.3 ~ 71.8%) compared with curcumin (47.3 %). From the test results we concluded that the length of methylene chain and different tertiary amine units did not make much contribution to the self-induced Aβ_{1-42} aggregation.

<center><Insert **Table 3**></center>

*2.2.5. Molecular modeling studies of **23c**.* In order to investigate the interaction mode of promising compound **23c** for AChE and BuChE, further molecular docking study was performed using the docking program, AutoDock 4.2 package with Discovery Studio 2.0, based on the X-ray crystal structure of AChE (PDB code: 1eve) and BuChE (PDB code: 4tpk) [27, 28]. The results showed that compound **23c** occupied the entire (catalytic active site) CAS, the mid-gorge sites and the peripheral anionic site (PAS) of AChE (**Fig. 3**), the benzene ring of chalcone skeleton interacted with key amino acid Phe330 via π-π interaction, two σ-π interactions with Trp84and one intermolecular hydrogen bonding interaction with Phe288. Moreover, hydrophobic interactions could be observed between the ligand and Asp72, Trp84, Gly118, Gly117, Phe330, Tyr334, Phe290, Phe331, Phe288, Trp279. Besides, compound **23c** interacted with BuChE via multiple sites (**Fig. 4**), the hydroxyl group and carbonyl of chalcone skeleton was involved in a hydrogen bond with Pro285. In addition, the key amino acid Tyr332 could interact with chalcone skeleton via one σ-π interaction and one π-π interaction, respectively. And the pyrrole ring could interact with Thr120 via one intermolecular hydrogen bonding. Besides, hydrophobic interactions could be observed between the ligand and Thr120, Asp70, Gly116, Phe329, Ala328, Tyr332, Trp82, His438. Based on these results observed, it could provide rational explanation for the high activity in inhibiting BuChE and AChE of **23c**.

<center><Insert **Fig. 3**></center>

<center><Insert **Fig. 4**></center>

Further molecular docking experiment was conducted on **23c** to explore the possible interacting mode with Aβ. The protein complex was downloaded from the Protein Data Bank (PDB: 1BA4). As shown in **Fig. 5**, the benzene ring of chalcone skeleton interacted with key amino acid Phe20 via π-π interaction, and the hydroxyl group of **23c** interacted with ASP1 *via* two intermolecular hydrogen bonding. Moreover, hydrophobic interactions were observed between the ligand and Asp1, Phe20, Asp23, and Phe19. These interactions might be favorable for the binding

of Aβ and compound **23c**.

<Insert **Fig. 5**>

In addition, molecular docking simulations of **23c** with MAO-B were carried out based on the X-ray crystal structures of human MAO-B (PDB code: 2V60). As shown in **Fig. 6**, the *O*-alkylamine side chain of **23c** was located in the well-known binding pocket of *hu*MAO-B, in close proximity to the enzymatic cofactor FAD. The hydroxyl group of chalcone skeleton interacted with Ile198 and Gln206 via intermolecular hydrogen bonding interaction, respectively, and the carbonyl group could also interact with Ile199 and Cys172 via intramolecular hydrogen bonding interaction, respectively. Moreover, the benzene ring of chalcone skeleton interacted with Tyr398 and Tyr435 via π-π interaction, respectively. Meanwhile, hydrophobic interactions could be observed between the ligand and Cys172, Tyr398, Tyr435, Gln206, Ile198, Ile199, Ile316, Pro102, Leu88. Thus, the results observed might provide the rational explanation for the MAO-B inhibitory activity of **23c**.

<Insert **Fig. 6**>

2.2.6. Metal-chelating properties of compounds 23c. We further tested the ability of compound **23c** to chelate biometals including Cu^{2+}, Zn^{2+}, Al^{3+} and Fe^{2+}. The experiment was conducted by UV-vis spectrophotometer [33]. The results showed that the maximum absorption wavelength of **23c** shifted from 361 nm to 422 nm after adding $CuCl_2$, indicating the formation of **23c**-Cu^{2+} complex (**Fig. 7**). Conversely, the maximum absorption exhibited no significant shift when $AlCl_3$, $ZnCl_2$ and $FeSO_4$ was added. These results indicated that the compound **23c** could selectively chelate with Cu^{2+}.

<Insert **Fig. 7**>

Next, we determined the stoichiometry of the **23c**-Cu^{2+} complex by the molar ratio method. The absorbance of the **23c** and $CuCl_2$ complexes at different concentrations at 422 nm was determined by ultraviolet spectroscopy. As seen from **Fig. 8**, the absorbance first increased linearly and then tended to be stable. These two lines intersected at a mole fraction of 1.06, showing a stoichiometric ratio of the composite **23c**-Cu^{2+} complex of 1:1.

<Insert **Fig. 8**>

2.2.7. Effects on Cu^{2+}-induced Aβ_{1-42} aggregation and disaggregation. To evaluate the Aβ aggregation ability of chalcone-*O*-alkylamines derivatives, Cu^{2+}-induced Aβ_{1-42} aggregation and the disaggregation assay were carried out using ThT binding assay [27]. Some of the target com-

pounds **20c, 20d, 21b, 21c, 21d, 22b, 22c, 23b, 23c** and **23d** were selected to test inhibition potency on Cu^{2+}-induced $A\beta_{1-42}$ aggregation, and curcumin.was also tested as positive compound. As shown in **Table 2**, most of the tested compounds showed better inhibition rate than curcumin (76.5%). The methylene chain and terminal group NR_1R_2 did not obviously affect the inhibition, and compound **23c** demonstrated good inhibition potency (81.2%).

For disaggregation effects on Cu^{2+}-induced $A\beta_{1-42}$ aggregation. According to the data, the representative compound **23c** displayed better disaggregation potency with 70.4% disaggregation ratio than curcumin (56.5%). The results displayed that compound **23c** could inhibit and disaggregate Cu^{2+}-induced *$A\beta_{1-42}$ aggregation*

2.2.8. Effect on abundance of Aβ fibrils by compound 23c. To complement the ThT assay, $A\beta_{1-42}$ aggregation was further probed by transmission electron microscopy (TEM) (**Fig. 9**). For inhibition assay in **Fig. 9B**, the fresh $A\beta_{1-42}$ had aggregated into amyloid fibrils after adding 25 μM Cu^{2+} during 24 h incubation, while the fresh $A\beta_{1-42}$ was treated with **23c** and Cu^{2+}, under the same experiments, small bulk aggregates were observed, implying that compound **23c** could inhibit Cu^{2+}-induced $A\beta_{1-42}$ aggregation. As for disaggregation assay, **Fig. 9D** displayed that the well-defined $A\beta_{1-42}$ fibrils obviously decreased after adding **23c** for another 24 h incubation, suggesting that **23c** could decompose the structure of Cu^{2+}-mediated $A\beta$ aggregation fibrils. Therefore, the TEM phenomenon further supported the conclusion that **23c** could inhibit and disaggregate Cu^{2+}-induced $A\beta_{1-42}$ aggregation fibrils.

<Insert **Fig. 9**>

2.2.9. Neuroprotective effects on H₂O₂-induced PC12 cell injury. The protective effects of **23c** against H_2O_2 injury were assessed using the 3-(4,5-dimethylthiazol-2-yl)-2,5- diphenyltetrazolium (MTT) assay [33]. According to the test results, **23c** did not show modified cell viability up to the concentration of 10 μM. With increased concentration to 100 μM, **23c** induced a decrease of cell viability (84.7%). The cell viability as determined by MTT reduction was remarkably declined after 100 μM H_2O_2 exposure, indicating significant sensitivity to H_2O_2-induced injury (**Fig. 10A**). However, treatment with compound **23c,** a significant dose-dependent protection was observed on H_2O_2-induced PC12 cell injury. Compound **23c** showed significant neuroprotective effect with 87.1% cell viability at 10.0 μM, and when the concentration of inhibitor **23c** was 1.0 μM, the cell viabilities dropped to 63.8% (**Fig. 10B**). This result indicated that compound **23c** could protected H_2O_2-induced PC12 cell injury.

<Insert **Fig. 10**>

2.2.10. In vitro blood–brain barrier permeation assay. One of the key requirements for successful central nervous system (CNS) drugs is the ability to cross BBB and having high brain penetration. For further evaluating the BBB penetration of compound **23c**, the parallel artificial membrane permeation assay of BBB (PAMPA-BBB) was performed [34, 35]. We compared the permeability of 11 commercial drugs with the reported values and verified the effectiveness of the assay (**Table S1**). The results showed that our experimental versus literature values have a good linear correlation (**Figure S1**). Taking into consideration of the limits established by Di et al's for the BBB penetration [35], we determined that compounds with effective permeation (Pe) values above 3.44×10^{-6} cm/s could cross the BBB (**Table S2**). The measured permeability showed that the Pe value of **23c** was $9.68 \pm 0.57 \times 10^{-6}$ cm/s, which could cross the BBB *in vitro*.

2.2.11 In vivo assay. The acute toxicity of **23c** was tested using Kunming mice at doses of 100, 250 and 500 mg/kg (n = 10 per group). The mice were observed continuously for the first 4 h through 14 days after oral administration of **23c**. The results showed compound **23c** did not show any acute toxicity and well tolerated at doses of up to 500 mg/kg. On this basis, the step-down passive avoidance task was carried out to evaluate whether **23c** could improve scopolamine-induced memory impairment [28, 36]. Results showed in **Fig. 11**, treatment with scopolamine (3 mg/kg) alone, the step-down latency remarkably declined to 65.8 sec ($p < 0.01$) compared with normal group (162.1 sec), while treatment with 5 mg/kg donepezil, the latency time rose to 156.5 sec ($p < 0.01$) compared with model group. Moreover, administration of compound **23c** (14.8, 7.4 and 3.7 mg/kg), the latency time gradually increased in a dose-dependent manner. In addition, the high dose group (14.8 mg/kg) of **23c** showed the highest latency time (141.9 s, $p < 0.05$) among the three dose groups, but displayed lower latency time than that of donepezil group (5 mg/kg, 156.5 sec). Therefore, compound **23c** could improve scopolamine-induced memory impairment to some extent.

<Insert **Fig. 11**>

3. Conclusion

In conclusion, we had designed and synthesized a series of chalcone-*O*-alkylamine derivatives as multifunctional agents for the treatment of AD. All the synthesized compounds were evaluated by AChE and BuChE inhibition, antioxidant activity, MAO-A/MAO-B inhibition and self-induced A$\beta_{1\text{-}42}$ aggregation inhibition *in vitro*. Among these synthesized compounds,

compound **23c** exhibited the best inhibitory potency of AChE and BuChE inhibition, good antioxidant activity, potential selective MAO-B inhibitory activities, and was able to inhibit self-induced Aβ_{1-42} aggregation. In addition, compound **23c** was a selective metal chelator, and could inhibit and decompose Cu^{2+}-induced Aβ_{1-42} aggregation. Both the TEM images and docking studies provided reasonable explain. Moreover, **23c** could cross the BBB *in vitro*. The further *in vivo* assay displayed that compound **23c** could improve scopolamine-induced memory impairment. Taken together, these results suggested that compound **23c** might be a potential multifunctional agent for the treatment of AD. Further studies to evaluate **23c** *in vivo* are in progress.

4. Experiment section

4.1. Chemistry

Unless otherwise noted, all materials (reagent grade) were purchased from commercial suppliers and used without further purification. The ^{1}H NMR and ^{13}C NMR spectra were recorded in CDCl$_3$ at 25 °C and referenced to tetramethylsilane (TMS) using a Bruker 400 NMR spectrometer. Mass spectra were obtained on an Agilent-6210 TOF LC-MS Spectrometer. The purities of all final compounds used for biological evaluation were determined by waters 2695 High Performance Liquid Chromatography (HPLC) with a Waters XBridge C18 column (4.6mm × 150 mm, 5 μm) at a flow rate of 1.0 mL/min. Mobile phase: A: 0.1%TFA in H$_2$O, B: 0.1% TFA in acetonitrile. The purity of all compounds was higher than 95%. Reaction progress was monitored by thin-layer chromatography (TLC) on silica gel GF254 plates from Qingdao Haiyang Chemical Co. Ltd. (China), the spots were detected under an UV lamp (254 nm).

4.1.1. General procedures for the synthesis of compounds *3-6*.

Compounds **3-6** were prepared according to our previously described procedure [37].

4.1.2. General procedure for the synthesis of compounds *7-10*.

Compounds **7-10** were prepared according to our previously described procedure [37].

4.1.3. General procedure for the synthesis of compounds *12-15*.

Compounds **12-15** were prepared refer to the literature and according to our previously described procedure [27, 38].

4.1.4. General procedure for the synthesis of compounds *16-19*.

Compounds **16-19** were prepared refer to the literature and according to our previously described procedure [27].

4.1.5. General procedure for the synthesis of compounds 20-23, 26a and 26b.

To a mixture of **7-10** or **25** (2 mmol) and the compounds **16-19** or **24** (2.5 mmol) in EtOH (7 mL) was added an aqueous solution of potassium hydroxide (50%, 6.5 mmol) at 0 °C. The mixture was stirred at room temperature for 48 hours, the reaction was monitored by TLC, then ice-cold water was poured into the solution and acidified with 10% HCl to pH = 3, and then the mixture was adjusted pH =8 using $NaHCO_3$ power. The mixture was extracted with CH_2Cl_2 (30 mL × 3), the organic phase was evaporated under reduced pressure. The residue was purified using mixtures of CH_2Cl_2/acetone (100:1) as eluent on a silica gel chromatography to obtain the products **20-23**, **26a** and **26b**.

(E)-1-(4-(2-(diethylamino)ethoxy)-2-hydroxyphenyl)-3-(4-(2-(diethylamino)ethoxy)phenyl)prop-2-en-1-one (20a). Light yellow oil; Yield: 59.1%; Purity: 97.25% (HPLC). ^{1}H NMR (400 MHz, CDCl$_3$) ^{1}H NMR (400 MHz, CDCl$_3$) δ 13.57 (s, 1H, Ar–OH), 7.92 – 7.81 (m, 2H, C=CH, Ar–H), 7.66 – 7.59 (m, 2H, 2 × Ar–H), 7.48 (d, J = 15.4 Hz, 1H, C=CH), 7.00 – 6.93 (m, 2H, 2 × Ar–H), 6.54 – 6.46 (m, 2H, 2 × Ar–H), 4.13 (t, J = 6.2 Hz, 4H, 2 × OCH$_2$), 2.93 (t, J = 6.1 Hz, 4H, 2 × CH$_2$), 2.74 – 2.62 (m, 8H, 4 × CH$_2$), 1.16 – 1.06 (m, 12H, 4 × CH$_3$). ^{13}C NMR (100 MHz, CDCl$_3$) δ 191.8, 166.5, 165.3, 161.1, 144.36, 131.1, 130.46, 127.5, 117.8, 115.0, 114.26, 108.0, 101.7, 66.9, 66.7, 51.6, 51.4, 47.9, 11.8, 11.8. HRMS (ESI): Cacld for (C$_{43}$H$_{50}$N$_2$O$_4$) requires: m/z 659.3804, found: 659.3847.

(E)-1-(2-hydroxy-4-(2-(pyrrolidin-1-yl)ethoxy)phenyl)-3-(4-(2-(pyrrolidin-1-yl)ethoxy)phenyl)prop-2-en-1-one (20b). Light yellow oil; Yield: 57.2%; Purity: 97.21% (HPLC). ^{1}H NMR (400 MHz, CDCl$_3$) δ 13.56 (s, 1 H, Ar–OH), 7.88 (d, J = 15.4 Hz, 1H, C=CH), 7.85 (d, J = 4.0 Hz, 1H, Ar–H), 7.65 – 7.58 (m, 2H, 2 × Ar–H), 7.47 (d, J = 15.4 Hz, 1H, C=CH), 7.35 – 7.25 (m, 4 H, 4 × Ar–H), 7.25 – 7.14 (m, 6H, 6 × Ar–H), 6.99 – 6.92 (m, 2 H, 2 × Ar–H), 6.55 – 6.44 (m, 2H, 2 × Ar–H), 4.20 – 4.16 (m, 4H, 2 × OCH$_2$), 3.09 – 2.96 (m, 4H, 2 × phCH$_2$), 2.84 (q, J = 5.6 Hz, 4H, 2 × CH$_2$), 2.57 (d, J = 7.0 Hz, 4H, 2 × CH$_2$), 2.16 – 2.03 (m, 4 H, 2 × CH$_2$), 1.74 – 1.64 (m, 4H, 2 × CH$_2$), 1.63 – 1.53 (m, 2 H, 2 × CH), 1.48 – 1.31 (m, 4 H, 2 × CH$_2$). ^{13}C NMR (100 MHz, CDCl$_3$) δ 191.8, 166.5, 165.3, 161.0, 144.2, 131.1, 130.3, 130.28, 127.7, 127.6, 117.8, 115.0, 114.87, 114.28, 108.07, 101.79, 67.4, 67.26, 54.9, 54.7, 54.7, 23.5. HRMS (ESI): Cacld for (C$_{29}$H$_{38}$N$_2$O$_4$) requires: m/z 479.2865, found: 479.2896.

(E)-1-(2-hydroxy-4-(2-(piperidin-1-yl)ethoxy)phenyl)-3-(4-(2-(piperidin-1-yl)ethoxy)phenyl)prop-2-en-1-one (20c). Light yellow oil; Yield: 51.1%; Purity: 97.05% (HPLC). ^{1}H NMR (400 MHz, CDCl$_3$) δ 13.53 (s, 1 H, Ar–OH), 7.87 – 7.77 (m, 2 H, C=CH, Ar–H), 7.58 (d, J = 8.5 Hz, 2 H, 2 × Ar–H), 7.43 (d, J = 15.4 Hz, 1 H, C=CH), 6.94 (dd, J = 8.7, 6.6 Hz, 2 H, 2 × Ar–H), 6.51 – 6.43 (m, 2 H, 2 × Ar–H), 4.14 (t, J = 6.1 Hz, 4 H, 2 × OCH$_2$), 2.75 – 2.80 (m, 4 H, 2 × CH$_2$), 2.51 (q, J = 5.4 Hz, 8H, 4 × CH$_2$), 1.64 – 1.59 (m, 8H, 4 × CH$_2$), 1.48 – 1.51 (m, 4H, 2 × CH$_2$). ^{13}C NMR (100 MHz, CDCl$_3$) δ 191.8, 190.8, 166.5, 165.2, 161.0, 144.2, 131.1, 130.45, 128.7, 128.5, 127.7, 127.6, 117.8, 115.1, 114.8, 114.6, 114.2, 110.6, 107.9, 101.8, 101.5, 79.7, 66.4, 66.2, 66.1, 65.9, 57.7, 57.6, 57.5, 55.0, 55.0, 55.0, 44.1, 29.7, 25.8, 25.8, 25.8, 25.7, 24.1, 24.1. HRMS (ESI): Cacld for (C$_{27}$H$_{34}$N$_2$O$_4$) requires: m/z 451.2552, found: 451.2598

(E)-1-(4-(2-(4-benzylpiperidin-1-yl)ethoxy)-2-hydroxyphenyl)-3-(4-(2-(4-benzylpiperidin-1-yl)ethoxy)phenyl)prop-2-en-1-one (20d). Light yellow oil; Yield: 49.1%; Purity: 97.82% (HPLC). ^{1}H NMR (400 MHz, CDCl$_3$) δ 13.56 (s, 1H, Ar–OH), 7.88 (d, J = 15.4 Hz, 1H, C=CH), 7.85 (d, J = 4.0 Hz, 1H, Ar–H), 7.65 – 7.58 (m, 2H, 2 × Ar–H), 7.47 (d, J = 15.4 Hz, 1H, C=CH), 7.35 – 7.25 (m, 4H, 4 × Ar–H), 7.25 – 7.14 (m, 6H, 6 × Ar–H), 6.99 – 6.92 (m, 2H, 2 × Ar–H), 6.55 – 6.44 (m, 2H, 2 × Ar–H), 4.18 (m, 4H, 2 × OCH$_2$), 3.09 – 2.96 (m, 4H, 2 × phCH$_2$), 2.84 (q, J = 5.6 Hz, 4H, 2 × CH$_2$), 2.57 (d, J = 7.0 Hz, 4H, 2 × CH$_2$), 2.16 – 2.03 (m, 4H, 2 × CH$_2$), 1.74 – 1.64 (m, 4H, 2 × CH$_2$), 1.63 – 1.53 (m, 2H, 2 × CH), 1.48 – 1.31 (m, 4H, 2 × CH$_2$). ^{13}C NMR (100 MHz, CDCl$_3$) δ 191.8, 166.5, 165.3, 161.0, 144.2, 131.1, 130.3, 130.2, 127.7, 127.6, 117.8, 115.0, 114.8, 114.2, 108.0, 101.7, 67.4, 67.2, 54.9, 54.7, 54.7, 23.5. HRMS (ESI): Cacld for (C$_{27}$H$_{38}$N$_2$O$_4$) requires: m/z 455.2865, found: 455.2911.

(E)-1-(4-(3-(diethylamino)propoxy)-2-hydroxyphenyl)-3-(4-(3-(diethylamino)propoxy)phenyl)prop-2-en-1-one (21a). Light yellow oil; Yield: 49.5%; Purity: 98.77% (HPLC). ^{1}H NMR (400 MHz, CDCl$_3$) δ 13.57 (s, 1H, Ar–OH), 7.90 – 7.80 (m, 2H, C=CH, Ar–H), 7.65 – 7.58 (m, 2H, 2 × Ar–H), 7.47 (d, J = 15.4 Hz, 1H, C=CH), 6.97 – 6.93 (m, 2H, 2 × Ar–H), 6.49 (d, J = 8.7 Hz, 2H, 2 × Ar–H), 4.09 (t, J = 6.2 Hz, 4H, 2 × OCH$_2$), 2.73 – 2.59 (m, 12H, 6 × CH$_2$), 2.06 – 1.95 (m, 4H, 2 × CH$_2$), 1.12 – 1.05 (m, 12H, 4 × CH$_3$). ^{13}C NMR (100 MHz, CDCl$_3$) δ 191.8, 166.6, 165.5, 161.2, 144.3, 131.1, 130.4, 127.4, 117.7, 114.9, 114.1, 107.8, 101.6, 66.6, 66.4, 49.3, 49.2, 47.0, 31.9, 31.5, 29.7, 29.4, 26.6, 26.5, 22.7, 14.2, 11.5, 11.4. HRMS (ESI): Cacld for (C$_{45}$H$_{54}$N$_2$O$_4$) requires: m/z 687.4117, found: 687.4149.

(E)-1-(2-hydroxy-4-(3-(pyrrolidin-1-yl)propoxy)phenyl)-3-(4-(3-(pyrrolidin-1-yl)propoxy)phenyl) *prop-2-en-1-one (21b).* Light yellow oil; Yield: 55.3%; Purity: 96.81% (HPLC). ^{1}H NMR (400 MHz, CDCl$_3$) δ 13.55 (s, 1H, Ar–OH), 7.87 – 7.79 (m, 2H, C=CH, Ar–H), 7.59 (dt, J = 8.9, 2.2 Hz, 2H, 2 × Ar–H), 7.45 (d, J = 15.4 Hz, 1H, C=CH), 6.99 – 6.91 (m, 2H, 2 × Ar–H), 6.54 – 6.44 (m, 2H, 2 × Ar–H), 4.20 – 4.14 (m, 4H, 2 × OCH$_2$), 2.97 – 2.90 (m, 4H, 2 × CH$_2$), 2.71– 2.58 (m, 12H, 6 × CH$_2$), 1.88– 1.77 (m, 12H, 6 × CH$_2$). ^{13}C NMR (100 MHz, CDCl$_3$) δ 191.8, 168.5, 166.5, 165.2, 161.0, 144.2, 131.1, 130.4, 130.2, 127.7, 127.5, 117.8, 115.0, 114.8, 114.8, 114.2, 108.0, 101.7, 101.5, 67.3, 67.1, 67.0, 55.0, 54.9, 54.7, 54.7, 44.1, 29.7, 23.5. HRMS (ESI): Cacld for (C$_{31}$H$_{42}$N$_2$O$_4$) requires: m/z 507.3178, found: 507.3216.

(E)-1-(2-hydroxy-4-(3-(piperidin-1-yl)propoxy)phenyl)-3-(4-(3-(piperidin-1-yl)propoxy)phenyl)p *rop-2-en-1-one (21c).* Light yellow oil; Yield: 56.4%; Purity: 96.47% (HPLC). ^{1}H NMR (400 MHz, CDCl$_3$) δ 13.57 (s, 1H, Ar–OH), 7.92 – 7.81 (m, 2H, C=CH, Ar–H), 7.62 (d, J = 8.4 Hz, 2H, 2 × Ar–H), 7.47 (d, J = 15.3 Hz, 1H, C=CH), 6.95 (d, J = 8.4 Hz, 2H, 2 × Ar–H), 6.49 (d, J = 8.5 Hz, 2H, 2 × Ar–H), 4.09 (t, J = 6.3 Hz, 4H, 2 × OCH$_2$), 2.62 – 2.47 (m, 12H, 6 × CH$_2$), 2.15 – 2.01 (m, 4H, 2 × CH$_2$), 1.73 – 1.73 (m, 8H, 4 × CH$_2$). ^{13}C NMR (100 MHz, CDCl$_3$) δ 191.8, 166.6, 165.4, 161.2, 144.3, 131.1, 130.4, 127.5, 117.7, 115.0, 114.1, 107.9, 101.6, 66.7, 66.5, 55.8, 55.7, 54.5, 54.5, 29.7, 26.3, 26.3, 25.6, 25.5, 24.2, 24.1. HRMS (ESI): Cacld for (C$_{29}$H$_{38}$N$_2$O$_4$) requires: m/z 479.2865, found: 479.2899.

(E)-1-(4-(3-(4-benzylpiperidin-1-yl)propoxy)-2-hydroxyphenyl)-3-(4-(3-(4-benzylpiperidin-1-yl)p *ropoxy)phenyl)prop-2-en-1-one (21d).* Light yellow oil; Yield: 58.6%; Purity: 97.22% (HPLC). ^{1}H NMR (400 MHz, CDCl$_3$) δ 13.53 (s, 1H, Ar–OH), 7.88 (d, J = 15.4 Hz, 1H, C=CH), 7.85 (d, J = 4.0 Hz, 1H, Ar–H), 7.65 – 7.59 (m, 2H, 2 × Ar–H), 7.47 (d, J = 15.4 Hz, 1H, C=CH), 7.35 – 7.25 (m, J = 7.3 Hz, 4H, 4 × Ar–H), 7.23 (dd, J = 7.4, 1.6 Hz, 2H, 2 × Ar–H), 6.96 – 6.91 (m, 2H, 2 × Ar–H), 6.50 – 6.44 (m, 2H, 2 × Ar–H), 4.15 – 6.05 (m, 4H, 2 × OCH$_2$), 3.28 – 3.11 (m, 4H, 2 × phCH$_2$), 2.85 – 2.68 (m, 4H, 2 × CH$_2$), 2.60 (q, J = 2.6 Hz, 4H, 2 × CH$_2$), 2.30 – 2.10 (m, 8H), 1.80 – 1.71 (m, 4H, 2 × CH$_2$), 1.69 – 1.53 (m, 6H, 3 × CH$_2$). ^{13}C NMR (100 MHz, CDCl$_3$) δ 191.9, 144.3, 131.3, 130.4, 129.1, 128.4, 127.8, 126.2, 117.9, 114.9, 114.4, 101.8, 42.3, 31.9, 31.7, 31.5, 31.5, 30.3, 30.2, 30.2, 29.7, 29.7, 29.5, 29.4, 27.2, 22.7, 14.14. HRMS (ESI): Cacld for (C$_{29}$H$_{42}$N$_2$O$_4$) requires: m/z 483.3178, found: 483.3221.

(E)-1-(4-(4-(diethylamino)butoxy)-2-hydroxyphenyl)-3-(4-(4-(diethylamino)butoxy)phenyl)prop- *2-en-1-one (22a).* Light yellow oil; Yield: 54.9%; Purity: 98.07% (HPLC). ^{1}H NMR (400 MHz,

CDCl$_3$) δ 13.58 (s, 1H, Ar–OH), 7.91 – 7.82 (m, 2H, C=CH, Ar–H), 7.65 – 7.59 (m, 2H, 2 × Ar–H), 7.48 (d, J = 15.4 Hz, 1H, C=CH), 6.98 – 6.92 (m, 2H, 2 × Ar–H), 6.51 – 6.46 (m, 2H, 2 × Ar–H), 4.05 (t, J = 6.4 Hz, 4H, 2 × OCH$_2$), 2.64 – 2.51 (m, 12H, 6 × CH$_2$), 1.88 – 1.79 (m, 4H, 2 × CH$_2$), 1.71 – 1.65 (m, 4H, 2 × CH$_2$), 1.09 – 1.05 (m, 12H, 4 × CH$_3$). ^{13}C NMR (100 MHz, CDCl$_3$) δ 191.8, 166.6, 165.6, 161.3, 144.3, 131.1, 130.4, 127.7, 127.4, 117.7, 115.0, 114.7, 114.1, 108.0, 101.5, 68.2, 68.0, 52.5, 52.4, 46.8, 46.2, 31.9, 31.7, 31.5, 31.5, 30.3, 30.2, 29.7, 29.6, 29.4, 29.0, 27.2, 27.1, 23.4, 23.4, 22.7, 14.1, 11.5, 11.5, 10.7. HRMS (ESI): Cacld for (C$_{47}$H$_{58}$N$_2$O$_4$) requires: m/z 715.4430, found: 715.4465.

(E)-1-(2-hydroxy-4-(4-(pyrrolidin-1-yl)butoxy)phenyl)-3-(4-(4-(pyrrolidin-1-yl)butoxy)phenyl)prop-2-en-1-one (22b). Light yellow oil; Yield: 57.4%; Purity: 96.77% (HPLC). ^{1}H NMR (400 MHz, CDCl$_3$) δ13.58 (s, 1H, Ar–OH), 7.90 – 7.83 (m, 2H, C=CH, Ar–H), 7.62 (d, J = 8.3 Hz, 2H, 2 × Ar–H), 7.48 (d, J = 15.3 Hz, 1H, C=CH), 6.95 (d, J = 8.3 Hz, 2H, 2 × Ar–H), 6.49 (d, J = 10.7 Hz, 2H, 2 × Ar–H), 4.06 (t, J = 6.3 Hz, 4H, 2 × OCH$_2$), 2.69 – 2.51 (m, 12H, 6 × CH$_2$), 1.94 – 1.67 (m, 16H, 8 × CH$_2$). ^{13}C NMR (100 MHz, CDCl$_3$) δ 191.8, 166.6, 165.5, 161.3, 144.3, 131.1, 130.4, 127.4, 117.7, 115.0, 114.1, 107.9, 101.6, 68.1, 67.9, 56.0, 56.0, 54.1, 31.9, 31.7, 31.5, 31.4, 30.3, 30.2, 30.2, 29.7, 29.7, 29.6, 29.5, 29.4, 29.2, 27.2, 27.1, 25.3, 25.3, 23.4, 22.7, 14.1. HRMS (ESI): Cacld for (C$_{33}$H$_{46}$N$_2$O$_4$) requires: m/z 535.3491, found: 535.3516.

(E)-1-(2-hydroxy-4-(4-(piperidin-1-yl)butoxy)phenyl)-3-(4-(4-(piperidin-1-yl)butoxy)phenyl)prop-2-en-1-one (22c). Light yellow oil; Yield: 51.1%; Purity: 97.26% (HPLC). ^{1}H NMR (400 MHz, CDCl$_3$) δ 13.58 (s, 1H, Ar–OH), 7.91 – 7.81 (m, 2H, C=CH, Ar–H), 7.66 – 7.59 (m, 2H, 2 × Ar–H), 7.47 (d, J = 15.3 Hz, 1H, C=CH), 6.97 – 6.92 (m, 2H, 2 × Ar–H), 6.51 – 6.44 (m, 2H, 2 × Ar–H), 4.05 (t, J = 6.1 Hz, 4H, 2 × OCH$_2$), 2.60 – 2.44 (m, 12H, 6 × CH$_2$), 1.90 – 1.73 (m, 8H, 4 × CH$_2$), 1.71 – 1.65 (m, 8H, 4 × CH$_2$), 1.53 – 1.46 (m, 4H, 2 × CH$_2$). ^{13}C NMR (100 MHz, CDCl$_3$) δ 191.8, 166.6, 165.5, 161.2, 144.3, 131.1, 130.4, 127.4, 117.7, 114.9, 114.1, 107.9, 101.5, 68.0, 67.8, 58.7, 54.4, 54.4, 29.7, 27.2, 27.1, 25.4, 25.4, 24.1, 24.1, 23.0. HRMS (ESI): Cacld for (C$_{31}$H$_{42}$N$_2$O$_4$) requires: m/z 507.3178, found: 507.3224.

(E)-1-(4-(4-(4-benzylpiperidin-1-yl)butoxy)-2-hydroxyphenyl)-3-(4-(4-(4-benzylpiperidin-1-yl)butoxy)phenyl)prop-2-en-1-one (22d). Light yellow oil; Yield: 60.1%; Purity: 97.73% (HPLC). ^{1}H NMR (400 MHz, CDCl$_3$) δ 13.57 (s, 1H, Ar–OH), 7.92 – 7.81 (m, 2H, C=CH, Ar–H), 7.66 – 7.58 (m, 2H, Ar–H), 7.48 (d, J = 15.4 Hz, 1H, C=CH), 7.31 (d, J = 7.5 Hz, 4H, 4 × Ar–H), 7.25 – 7.14 (m, 6H, 4 × Ar–H), 6.97 – 6.91 (m, 2H, 2 × Ar–H), 6.48 (d, J = 8.2 Hz, 2H, 2 × Ar–H), 4.05 (t,

J = 6.3 Hz, 4H, 2 × OCH$_2$), 3.05 – 2.87 (m, 4H, 2 × CH$_2$), 2.56 (d, J = 7.0 Hz, 4H, 2 × CH$_2$), 2.46 – 2.35 (m, 4H, 2 × CH$_2$), 1.91 (q, J = 9.4, 7.2 Hz, 4H, 2 × CH$_2$), 1.83 (q, J = 6.9 Hz, 4H, 2 × CH$_2$), 1.77 – 1.62 (m, 8H, 4 × CH$_2$), 1.60 – 1.51 (m, 2H, CH$_2$). ^{13}C NMR (100 MHz, CDCl$_3$) δ 191.8, 166.6, 165.5, 161.3, 144.3, 140.7, 140.6, 131.2, 130.4, 129.1, 128.2, 127.4, 125.8, 125.8, 117.7, 115.0, 114.1, 108.0, 101.6, 68.1, 67.9, 58.5, 58.5, 53.9, 43.2, 37.9, 32.1, 31.7, 29.7, 27.3, 27.1, 23.5, 23.4, 22.7, 14.2. HRMS (ESI): Cacld for (C$_{31}$H$_{46}$N$_2$O$_4$) requires: m/z 511.3491, found: 511.3534.

(E)-1-(4-((6-(diethylamino)hexyl)oxy)-2-hydroxyphenyl)-3-(4-((6-(diethylamino)hexyl)oxy)phenyl)prop-2-en-1-one (23a). Light yellow oil; Yield: 55.1%; Purity: 96.92% (HPLC). ^{1}H NMR (400 MHz, CDCl$_3$) δ 13.57 (s, 1H, Ar–OH), 7.90 – 7.80 (m, 2H, C=CH, Ar–H), 7.60 (dd, J = 8.8, 2.4 Hz, 2H, 2 × Ar–H), 7.46 (d, J = 15.4 Hz, 1H, C=CH), 6.93 (dd, J = 8.7, 2.4 Hz, 2H, 2 × Ar–H), 6.51 – 6.41 (m, 2H, 2 × Ar–H), 4.00 (t, J = 6.4 Hz, 4H, 2 × OCH$_2$), 2.73 (q, J = 7.2 Hz, 8H, 4 × CH$_2$), 2.67 – 2.58 (m, 4H, 2 × CH$_2$), 1.88 – 1.74 (m, 4H, 2 × CH$_2$), 1.61 (q, J = 8.2 Hz, 4H, 2 × CH$_2$), 1.50 (ddt, J = 14.0, 10.5, 5.9 Hz, 4H, 2 × CH$_2$), 1.41 (t, J = 8.6 Hz, 4H, 2 × CH$_2$), 1.31– 1.26 (m, 4H, 2 × CH$_2$), 1.16 (t, J = 7.2 Hz, 12H, 4 × CH$_3$). ^{13}C NMR (100 MHz, CDCl$_3$) δ 191.8, 166.5, 165.5, 161.3, 144.3, 131.2, 130.4, 127.7, 127.3, 123.9, 117.7, 114.9, 114.0, 107.9, 101.5, 68.1, 67.9, 52.1, 46.6, 31.9, 31.7, 31.4, 30.3, 30.2, 29.7, 29.6, 29.6, 29.3, 29.0, 28.8, 27.1, 27.0, 25.8, 25.8, 25.3, 22.7, 14.1, 10.3, 10.3, 10.2. HRMS (ESI): Cacld for (C$_{51}$H$_{66}$N$_2$O$_4$) requires: m/z 771.5056, found: 771.5089.

(E)-1-(2-hydroxy-4-((6-(pyrrolidin-1-yl)hexyl)oxy)phenyl)-3-(4-((6-(pyrrolidin-1-yl)hexyl)oxy)phenyl)prop-2-en-1-one (23b). Light yellow oil; Yield: 54.3%; Purity: 97.39% (HPLC). ^{1}H NMR (400 MHz, CDCl$_3$) δ 13.57 (s, 1H, Ar–OH), 7.92 – 7.81 (m, 2H, C=CH, Ar–H), 7.62 (d, J = 8.6 Hz, 2H, 2 × Ar–H), 7.48 (d, J = 15.4 Hz, 1H, C=CH), 6.95 (d, J = 8.5 Hz, 2H, 2 × Ar–H), 6.54 – 6.44 (m, 2H, 2 × Ar–H), 4.10– 4.01 (m, 4H, 2 × OCH$_2$), 2.70 – 2.51 (m, 12H, 6 × CH$_2$), 1.93 – 1.70 (m, 14H, 2 × CH$_2$), 1.68 – 1.57 (m, 2H, CH$_2$), 1.56 – 1.47 (m, 2H, CH$_2$), 1.47 – 1.39 (m, 2H, CH$_2$). ^{13}C NMR (100 MHz, CDCl$_3$) δ 191.8, 166.5, 165.6, 161.3, 144.2, 131.1, 130.3, 127.3, 117.7, 114.9, 114.0, 107.9, 101.5, 68.2, 67.9, 56.4, 56.0, 54.1, 29.7, 28.9, 28.4, 27.3, 27.2, 25.9, 25.3, 23.4, 23.4. HRMS (ESI): Cacld for (C$_{37}$H$_{54}$N$_2$O$_4$) requires: m/z 591.4117, found: 591.4139.

(E)-1-(2-hydroxy-4-((6-(piperidin-1-yl)hexyl)oxy)phenyl)-3-(4-((6-(piperidin-1-yl)hexyl)oxy)phenyl)prop-2-en-1-one (23c). Light yellow oil; Yield: 57.9%; Purity: 98.24% (HPLC). ^{1}H NMR (400 MHz, CDCl$_3$) δ13.58 (s, 1H, Ar–OH), 7.92 – 7.80 (m, 2H, C=CH, Ar–H), 7.62 (d, J = 8.4 Hz,

2H, 2 × Ar–H), 7.48 (d, J = 15.3 Hz, 1H, C=CH), 6.94 (d, J = 8.5 Hz, 2H, 2 × Ar–H), 6.53 – 6.44 (m, 2H, 2 × Ar–H), 4.04 (t, J = 6.2 Hz, 4H, 2 × OCH$_2$), 2.64 – 2.46 (m, 12H, 6 × CH$_2$), 1.88 – 1.64 (m, 20H, 10 × CH$_2$), 1.55 – 1.46 (m, 6H, 3 × CH$_2$), 1.42– 1.37 (m, 2H, CH$_2$). ^{13}C NMR (100 MHz, CDCl$_3$) δ 191.8, 166.6, 165.6, 161.3, 144.3, 131.1, 130.4, 127.4, 117.7, 114.9, 114.0, 107.9, 101.5, 68.2, 67.8, 58.8, 58.7, 54.4, 54.2, 31.9, 29.7, 28.8, 27.2, 27.2, 25.8, 25.4, 24.9, 24.1, 23.8, 23.0, 22.7, 14.1. HRMS (ESI): Cacld for (C$_{35}$H$_{50}$N$_2$O$_4$) requires: m/z 563.3804, found: 563.3847.

(E)-1-(4-((6-(4-benzylpiperidin-1-yl)hexyl)oxy)-2-hydroxyphenyl)-3-(4-((6-(4-benzylpiperidin-1-yl)hexyl)oxy)phenyl)prop-2-en-1-one (23d). Light yellow oil; Yield: 51.1%; Purity: 97.36% (HPLC). ^{1}H NMR (400 MHz, CDCl$_3$) δ 13.53 (s, 1H, Ar–OH), 7.90 – 7.79 (m, 2H, C=CH, Ar–H), 7.60 (dd, J = 8.7, Hz, 2H, 2 × Ar–H), 7.47 (d, J = 15.4 Hz, 1H, C=CH), 6.92 (dd, J = 8.7, 2.5 Hz, 2H, 2 × Ar–H), 6.52 – 6.40 (m, 2H, 2 × Ar–H), 4.12 – 3.95 (m, 4H, 2 × OCH$_2$), 3.53 – 3.40 (m, 4H, 2 × CH$_2$), 3.00 – 2.75 (m, 4H, 2 × CH$_2$), 2.67 – 2.46 (m, 10H, 5 × CH$_2$), 2.11 – 1.61 (m, 20H, 4 × CH$_2$, 4 × CH$_3$), 1.58 – 1.36 (m, 4H, 2 × CH$_2$). ^{13}C NMR (100 MHz, CDCl$_3$) δ 191.8, 166.5, 165.2, 161.0, 144.2, 131.1, 130.3, 130.2, 127.5, 117.8, 115.0, 114.8, 114.7, 114.2, 107.9, 101.7, 67.3, 67.1, 54.9, 54.9, 54.7, 54.7, 23.5, 22.7, 14.2. HRMS (ESI): Cacld for (C$_{35}$H$_{54}$N$_2$O$_4$) requires: m/z 567.4117, found: 567.4153.

(E)-1-(2-hydroxy-4-((6-(pyrrolidin-1-yl)hexyl)oxy)phenyl)-3-phenylprop-2-en-1-one (26a). Light yellow oil; Yield: 43.7%; Purity: 98.11% (HPLC). ^{1}H NMR (400 MHz, CDCl$_3$) δ 13.42 (s, 1H, Ar–OH), 8.07 (d, J = 7.2 Hz, 1H, Ar-H), 7.87 (d, J = 15.6 Hz, 1H, CH=CH), 7.83 (d, J = 9.2 Hz, 1H, Ar-H), 7.66-7.64 (m, 2H, 2 × Ar-H), 7.58 (d, J = 15.6 Hz, 1H, CH=CH), 7.43-7.38 (m, 2H, 2 × Ar-H), 6.47 (d, J = 8.8 Hz, 1H, Ar-H), 6.42 (s, 1H, Ar-H), 3.98 (t, J = 6.0 Hz, 2H, OCH$_2$), 3.30-3.27 (m, 4H, 2 × NCH$_2$), 3.04 (t, J = 8.0 Hz, 2H, NCH$_2$), 2.13-2.09 (m, 4H, 2 × CH$_2$), 1.93-1.87 (m, 2H, CH$_2$), 1.82-1.75 (m, 2H, CH$_2$), 1.52-1.44 (m, 4H, 2 × CH$_2$). ^{13}C NMR (100 MHz, CDCl$_3$) δ 191.8, 166.6, 165.7, 144.4, 134.7, 131.5, 131.4, 130.7, 129.6, 129.0, 128.5, 128.0, 120.3, 114.0, 108.0, 101.6, 68.0, 55.3, 53.5 (2C), 28.6, 26.5, 25.6, 25.4, 23.3 (2C). HRMS (ESI): Cacld for (C$_{25}$H$_{31}$NO$_3$) requires: m/z 394.2337, found: 394.2382.

(E)-1-(2-hydroxyphenyl)-3-(4-((6-(pyrrolidin-1-yl)hexyl)oxy)phenyl)prop-2-en-1-one (26b). Light yellow oil; Yield: 49.2%; Purity: 97.92% (HPLC). ^{1}H NMR (400 MHz, CDCl$_3$) δ 12.94 (s, 1H, Ar–OH), 7.93 (d, J = 8.8 Hz, 1H, Ar-H), 7.90 (d, J = 16.0 Hz, 1H, CH=CH), 7.62 (d, J = 8.4 Hz, 2H, 2 × Ar-H), 7.55 (d, J = 15.6 Hz, 1H, CH=CH), 7.49 (t, J = 7.6 Hz, 1H, Ar-H), 7.02 (d, J = 8.0 Hz, 1H, Ar-H), 6.98 (d, J = 9.2 Hz, 1H, Ar-H), 6.93 (d, J = 8.0 Hz, 2H, 2 × Ar-H), 4.01 (t, J = 6.0

Hz, 2H, OCH$_2$), 3.28-3.23 (m, 4H, 2 × NCH$_2$), 3.01 (t, J = 8.0 Hz, 2H, NCH$_2$), 2.15-2.12 (m, 4H, 2 × CH$_2$), 1.94-1.89 (m, 2H, CH$_2$), 1.84-1.80 (m, 2H, CH$_2$), 1.56-1.51 (m, 2H, CH$_2$), 1.50-1.45 (m, 2H, CH$_2$). ^{13}C NMR (100 MHz, CDCl$_3$) δ 193.7, 163.5, 161.5, 145.4, 136.2, 132.0, 130.6, 129.6, 127.3, 118.8, 118.6, 117.5, 115.0, 114.7, 67.8, 55.5, 53.6 (2C), 29.7, 28.8, 26.5, 25.7, 23.4 (2C). HRMS (ESI): Cacld for (C$_{25}$H$_{31}$NO$_3$) requires: m/z 394.2337, found: 394.2374.

4.2. Biological evaluation

4.2.1. AChE and BuChE inhibition assay

The modified Ellman method was used to determine the AChE and BuChE inhibitory ability of the compounds, using AChE from electric eel (Sigma-Aldrich Corporation) and human erythrocytes (Sigma-Aldrich Corporation) or BuChE from equinum serum (Sigma-Aldrich Corporation) and human serum (Sigma-Aldrich Corporation). Acetylthiocholine iodide (1 mmol/L, 30 μL), phosphate-buffered solution (0.1 mmol/L, pH = 8.0, 40 lL), ChE (0.05 U/mL, final concentration, 10 μL) and different concentrations of test compounds (20 μL) were used for the ChE inhibition assay. Blanks containing all components except ChE were carried out. IC$_{50}$ values were calculated as the concentration of compound that produces more than 50% AChE or BuChE activity inhibition. The detailed procedure refers to the literature and our previous work [28, 36].

4.2.2. In vitro inhibition of MAOs

To evaluate the MAOs inhibition activity of target compounds, recombinant human MAO-A and -B purchased from Sigma–Aldrich Co. were used. The detailed procedure refers to the literature and our previous work [39].

4.2.3. Molecular docking

The X-ray crystal structure of AChE (PDB code: 1eve), BuChE (PDB code: 4tpk), Aβ (PDB: 1BA4) and human MAO-B (PDB code: 2V60) was download from Protein Data Bank (www.rcsb.org) [39]. The AUTODOCK 4.2 program was used for the docking study of **23c**. Each docked system was performed by 200 runs of the Autodock search by the Lamarckian genetic algorithm (LGA). A cluster analysis was performed on the docking results using a root mean square (RMS) tolerance of 1.0 and the lowest energy conformation of the highest populated cluster was selected for analysis. Graphic manipulations and visualizations were done by Autodock Tools (ADT; version 1.5.6) or Discovery Studio 2.5 software.

4.2.4. Metal binding studies

The metal binding studies were performed with Varioskan Flash Multimode Reader (Thermo Scientific) [40]. After 30-minutes incubation in methanol at room temperature, the UV spectrum value with a wavelength in the range of 200-600 nm of **23c** was recorded with or without $CuCl_2$, $ZnCl_2$, $AlCl_3$ and $FeSO_4$. The final concentration of test compound and metal was 37.5 μM.

The stoichiometry of the compound-Cu^{2+} complex was determined by titrating the methanol solution of the test compounds with an increasing concentration of $CuCl_2$. The final concentration of the test compound was 37.5 μM and the final concentration of Cu^{2+} ranged from 3.75 to 93.75 μM. The molar fraction relative to the test compound was investigated by subtracting $CuCl_2$ and the corresponding concentration of test compound for recording and processing.

4.2.5 Antioxidant activity assay

The antioxidant activity of target compounds was devalued by the oxygen radical absorbance capacity fluorescein (ORAC-FL) assay [41]. All the assays were performed with 75mM phosphate buffer (pH = 7.40), and the final reaction mixture was 200 μL. FL (120 μL, 150 nM final concentration) and antioxidant (20 μL) were added in the wells of a black 96-well plate using Trolox as a standard (1-8 μM, final concentration). The details could reference our previous work [27, 28].

4.2.6 Self-induced $A\beta_{1\text{-}42}$ aggregation assay

The self-induced $A\beta_{1\text{-}42}$ aggregation was measured by a Thioflavin T-based (ThT) binding assay [42, 43]. Thioflavin T (Basic Yellow 1, ThT) was purchased from TCI (Shanghai) Development. β-Amyloid$_{1-42}$ ($A\beta_{1\text{-}42}$), supplied as trifluoroacetate salt, was purchased from ChinaPeptides Co., Ltd. 1,1,1,3,3,3-hexafluoro-2-propanol (HFIP) was purchased from Energy Chemical. Briefly, $A\beta_{1\text{-}42}$ was dissolved in 1 mg/mL of HFIP and incubated for 24 hours at room temperature. The dried $A\beta_{1\text{-}42}$ was then re-dissolved in DMSO to make a solution of 200 μM and maintained at -80 °C. Solutions of test compounds were prepared in DMSO in 2.5 mM for storage and diluted with phosphate buffer solution (pH 7.4) before use. $A\beta_{1\text{-}42}$ (20 μL, 25 μM, final concentration) was incubated with 20 μL of test compounds (25 μM, final concentration) in 50 mM phosphate buffer solution (pH 7.40) at 37 ° C for 24 h. After the incubation, 160 μL of 5 μM ThT in 50mM glycine-NaOH buffer (pH 8.0) was added to each well. Fluorescence was measured by a Varioskan Flash Multimode Reader (Thermo Scientific) with excitation and emission wavelengths of 446 and 490 nm, respectively.

4.2.7 Metal-induced $A\beta_{1\text{-}42}$ aggregation and disaggregation

Cu^{2+}-induced $A\beta_{1\text{-}42}$ aggregation was determined using ThT method [28]. Solutions of Cu^{2+} were prepared from standards to concentration of 75 μM HEPES buffer solution (20 mM, pH 6.6, 150 μM NaCl). The $A\beta_{1\text{-}42}$ stock solution was diluted in HEPES buffer (20 mM, pH 6.6, 150 μM NaCl). The mixture of $A\beta_{1\text{-}42}$ (20 μL, 25 μM, final concentration) and Cu^{2+} (20 μL, 25 μM, final concentration) with or without the tested compound (20 μL, 25 μM, final concentration) was incubated at 37 ° C for 24 h. After which, 190 μL of 5 μM ThT in 50 mM glycine-NaOH buffer (pH 8.50) was added. Each assay was performed in triplicate. The detection method was the same as the self-induced $A\beta_{1\text{-}42}$ experiment.

In the disaggregation of Cu^{+}-induced $A\beta_{1\text{-}42}$ fibrils experiment, $A\beta_{1\text{-}42}$ stock solutions were diluted in HEPES buffer (20 mM, pH = 6.6, 150 mM NaCl). A mixture of $A\beta_{1\text{-}42}$ (20 μL, 25 μM, final concentration and Cu^{2+} (20 μL, 25 μM, final concentration) was incubated for 24 hours at 37° C. 20 μL inhibitor (final concentration was 25 μM) was then added into the mixture of $A\beta_{1\text{-}42}$ with Cu^{2+} and incubated at 37 °C for another 24 hours. Heat-resistant plastic film was used to minimize evaporation effect. After which, glycine-NaOH buffer with 190 μL of 5 μM thioflavin T was added. Each assay was run in triplicate. The detection method was the same as the self-induced $A\beta_{1\text{-}42}$ experiment.

4.2.8 Hydrogen peroxide induced PC12 cell injury [27]

PC-12 cells were seeded into 96-well plates at a density of 1×10^5 cells per mL in DMEM medium (GIBCO.) supplemented with 10% heat-inactivated bovine calf serum (Hyclone). After incubation overnight, the medium was replaced with fresh DMEM medium without calf serum and phenol red. And tested compounds at various concentrations were added and incubated with the cells for further 2 h. Then the cells were treated with 100 μM H_2O_2 for 2 hours. For the control group, the cells were treated without H_2O_2 for 2 hours. At the end of the assay, the cells were incubated with 0.5 mg/mL 3-(4,5-dimethylthiazol-2-yl)-2,5-diphenyltetrazolium bromide (MTT) for 4 h at 37 ° C. The supernatants were carefully removed, and 150 μL DMSO was added into each well. The absorbance at 570 nm of the formazan was determined using a Varioskan Flash Multimode Reader (Thermo Scientific). Data were expressed as mean ± SD. To determine the cytotoxicity of the compound, tested compound was incubated with PC-12 cells for 48 h without the addition of H_2O_2, and other procedures were similar to the above mentioned.

4.2.9 In vitro blood−brain barrier permeation assay

As described by the literature [35], parallel artificial membrane permeation assay was used to evaluate the blood-brain barrier penetration of target compounds. The detailed procedure refers to our previous work [36].

4.2.10 In vivo assay

Kunming mice at body weight of 18–22 g (six weeks old, either gender) were supplied by the Center of Experimental Animals of Sichuan Academy of Chinese Medicine Sciences (eligibility certification no. SCXK[chuan] 2015-030). Mice were maintained under standard conditions with a 12 h:12 h light–dark cycle at 20–22 °C with a relative humidity of 60–70%. Sterile food and water were provided according to institutional guidelines.

Acute toxicity. Compound **23c** was suspended in 0.5% carboxymethylcellulose sodium (CMC-Na) salt solution (100, 250, 500 mg/kg) and given via oral administration according to the divided experimental groups. After the administration of the compound **23c**, the mice were observed continuously for the first 4 h for any abnormal behavior and mortality changes, intermittently for the next 24 h, and occasionally thereafter for 14 days for the onset of any delayed effects. All animals were sacrificed on the 14th day after drug administration and were macroscopically examined for possible damage to the heart, liver, and kidneys.

A step-down passive avoidance test was performed to test the ability of memory in mice [27, 36]. The apparatus consisted of a grid floor with a wooden block placed in the center. The block served as a shock free zone. The mice underwent two separate trials: a training trial and a test trial 24 h later. For training trial, mice were initially placed on the block and were given an electrical foot shock (0.5 mA, 2s) through the grid floor on stepping down. Compound **23c** (14.8, 7.4 and 3.7 mg/kg, *p.o.*) or donepezil (5.0 mg/kg, *p.o.*) as a positive control were orally given 1 h before each training trial. After 30 min, memory impairment was induced by administering scopolamine (3 mg/kg, *i.p.*). Twenty-four hours after the training trial, mice were placed on the block and the time for the animal to step down was measured as latency time for test trial. An upper cut-off time was set at 300 s.

All data are expressed as mean ± SEM. Differences between groups were examined for statistical significance using one-way ANOVA with Student's *t* test. A *P* value less than 0.05 denoted the presence of a statistically significant difference.

AUTHOR INFORMATION

Corresponding Author

* For Xiaoxia Lu: E-mail: luxx@cib.ac.cn

* For Zhipei Sang: E-mail: sangzhipei@126.com

Author Contributions

The manuscript was written through contributions of all authors. All authors have given approval to the final version of the manuscript. #These authors contributed equally.

Notes

The authors declare no competing financial interest.

Supporting Information Available:

Figures and Tables in PAMPA-BBB, and some representative ^{1}H, ^{13}C NMR, HR-ESI-MS and HPLC spectra for the synthesized compounds are available as supplementary material.

References

[1] Ballard C, Gauthier S, Corbett A, Brayne C, Aarsland D, Jones E. Alzheimer's disease. *Lancet* 2011, *377*(9770): 1019-1031.

[2] Prince, M., Comas-Herrera, A., Knapp, M., Guerchet, M., and Karagiannidou, M. (2016) World Alzheimer Report 2016. Improving healthcare for people living with dementia: Coverage, quality and costs now and in the future, Alzheimer's Disease International, London,

https://www.alz.co.uk/research/WorldAlzheimerReport2016.pdf

[3] Kumar A, Singh A, Ekavali. A review on Alzheimer's disease pathophysiology and its management: an update. *Pharmacological Reports,* 2015, 67(2): 195-203.

[4] Huang Y, Mucke L. Alzheimer mechanisms and therapeutic strategies. *Cell*, 2012, *148*(6): 1204-1222.

[5] Li X, Wang H, Lu Z, Zheng X, Ni W, Zhu J, Fu Y, Lian F, Zhang N, Li J, Zhang H, Mao F. Development of multifunctional pyrimidinylthiourea derivatives as potential anti-Alzheimer agents. *Journal of Medicinal Chemistry*, 2016, *59*(18): 8326-8344.

[6] Anand P, Singh B. A review on cholinesterase inhibitors for Alzheimer's disease. *Archives of Pharmacal Research*, 2003, *36*(4): 375-399.

[7] Hardy J, Selkoe D. J. The amyloid hypothesis of Alzheimer's disease: progress and problems on the road to therapeutics. *Science*, 2002, *297*(5580), 353-356.

[8] Liston, D. R., Nielsen, J. A., Villalobos, A., Chapin, D., Jones, S. B., Hubbard, S. T., White, W. F. Pharmacology of selective acetylcholinesterase inhibitors: implications for use in Alzheimer's disease. *European Journal of Pharmacology*, 2004, *486*(1), 9-17.

[9] Bartorelli, L., Giraldi, C., Saccardo, M., Cammarata, S., Bottini, G., Fasanaro, A. M. Effects of switching from an AChE inhibitor to a dual AChE-BuChE inhibitor in patients with Alzheimer's disease. *Current Medical Research and Opinion*, 2005, *21*(11): 1809-1817.

[10] Sun, K., Bai, Y., Zhao, R., Guo, Z., Su, X., Li, P., Yang, P. Neuroprotective effects of matrine on scopolamine-induced amnesia via inhibition of AChE/BuChE and oxidative stress. *Metabolic Brain Disease*, 2019, *34*(1): 173-181.

[11] Sánchez, L., Madurga, S., Pukala, T., Vilaseca, M., López-Iglesias, C., Robinson, C. V. Carulla, N. $A\beta_{40}$ and $A\beta_{42}$ amyloid fibrils exhibit distinct molecular recycling properties. *Journal of the American Chemical Society*, 2011, *133*(17): 6505-6508

[12] James, S. A., Churches, Q. I., de Jonge, M. D., Birchall, I. E., Streltsov, V., McColl, G., Hare, D. J. Iron, copper, and zinc concentration in Aβ plaques in the APP/PS1 mouse model of Alzheimer's disease correlates with metal levels in the surrounding neuropil. *ACS Chemical*

Neuroscience, 2016, *8*(3): 629-637.

[13] Soodi, M., Dashti, A., Hajimehdipoor, H., Akbari, S., Ataei, N. Melissa officinalis acidic fraction protects cultured cerebellar granule neurons against beta amyloid-induced apoptosis and oxidative stress. *Cell Journal (Yakhteh)*, 2017, *18*(4): 556-564.

[14] Cesari, N., Biancalani, C., Vergelli, C., Dal Piaz, V., Graziano, A., Biagini, P., Giovannoni, M. P. Arylpiperazinylalkylpyridazinones and analogues as potent and orally active antinociceptive agents: synthesis and studies on mechanism of action. *Journal of Medicinal Chemistry*, 2006, *49*(26): 7826-7835.

[15] Amin, F. U., Shah, S. A., & Kim, M. O. Vanillic acid attenuates Aβ 1-42-induced oxidative stress and cognitive impairment in mice. *Scientific Reports*, 2017, *7*, 40753.

[16] Kumar B, Gupta VP, Kumar V. A perspective on monoamine oxidase enzyme as drug target: challenges and opportunities. *Curr Drug Targets.* 2017, 18(1): 87-97.

[17] Carradori, S., Secci, D., Petzer, J. P. MAO inhibitors and their wider applications: a patent review. *Expert Opinion on Therapeutic Patents*, 2018, *28*(3): 211-226.

[18] Carradori, S., Silvestri, R. New frontiers in selective human MAO-B inhibitors: miniperspective. *Journal of Medicinal Chemistry*, 2015, *58*(17): 6717-6732.

[19] Agis-Torres, A., Sollhuber, M., Fernandez, M., Sanchez-Montero, J. M. Multi-target-directed ligands and other therapeutic strategies in the search of a real solution for Alzheimer's disease. *Current Neuropharmacology*, 2014, *12*(1): 2-36.

[20] Singh, M., Kaur, M., Chadha, N., & Silakari, O. Hybrids: a new paradigm to treat Alzheimer's disease. *Molecular diversity*, 2016, *20*(1): 271-297.

[21] Cavalli, A., Bolognesi, M. L., Minarini, A., Rosini, M., Tumiatti, V., Recanatini, M., Melchiorre, C. Multi-target-directed ligands to combat neurodegenerative diseases. *Journal of Medicinal Chemistry*, 2008, *51*(3): 347-372.

[22] Leon, R., Garcia, A. G, Marco Contelles, J. Recent advances in the multitarget⬜directed ligands approach for the treatment of Alzheimer's disease. *Medicinal research reviews*, 2013, *33*(1): 139-189.

[23] Sahu NK, Balbhadra SS, Choudhary J, Kohli DV. Exploring pharmacological significance of chalcone scaffold: a review. *Current Medicinal Chemistry*, 2012, *19*(2): 209-225.

[24] Gomes M, Muratov E, Pereira M, Peixoto J, Rosseto L, Cravo P, Andrade C, Neves B. Chalcone derivatives: promising starting points for drug design. *Molecules*. 2017, 22(8): pii: E1210.

[25] Choi, J. W., Jang, B. K., Cho, N. C., Park, J. H., Yeon, S. K., Ju, E. J., Park, K. D. Synthesis of a series of unsaturated ketone derivatives as selective and reversible monoamine oxidase inhibitors. *Bioorganic & Medicinal Chemistry*, 2015, *23*(19): 6486-6496.

[26] Li, Z., Cui, M., Dai, J., Wang, X., Yu, P., Yang, Y., Saji, H. Novel cyclopentadienyl tricarbonyl complexes of 99mTc mimicking chalcone as potential single-photon emission computed tomography imaging probes for β-amyloid plaques in brain. *Journal of Medicinal Chemistry*, 2013, *56*(2): 471-482.

[27] Sang, Z., Qiang, X., Li, Y., Yuan, W., Liu, Q., Shi, Y., Deng, Y. Design, synthesis and evaluation of scutellarein-O-alkylamines as multifunctional agents for the treatment of Alzheimer's disease. *European Journal of Medicinal Chemistry*, 2015, *94*, 348-366.

[28] Qiang, X., Sang, Z., Yuan, W., Li, Y., Liu, Q., Bai, P., Deng, Y. Design, synthesis and evaluation of genistein-O-alkylbenzylamines as potential multifunctional agents for the treatment of Alzheimer's disease. *European Journal of Medicinal Chemistry*, 2014, *76*, 314-331.

[29] Bolognesi, M. L., Chiriano, G., Bartolini, M., Mancini, F., Bottegoni, G., Maestri, V., Rosini, M. Synthesis of monomeric derivatives to probe memoquin's bivalent interactions. *Journal of Medicinal Chemistry*, 2011, *54*(24): 8299-8304.

[30] Bolognesi, M. L., Cavalli, A., Valgimigli, L., Bartolini, M., Rosini, M., Andrisano, V., Melchiorre, C. Multi-target-directed drug design strategy: from a dual binding site acetylcholinesterase inhibitor to a trifunctional compound against Alzheimer's disease. *Journal of Medicinal Chemistry*, 2007, *50*(26): 6446-6449.

[31] Cavalli, A., Bolognesi, M. L., Capsoni, S., Andrisano, V., Bartolini, M., Margotti, E. Melchiorre, C. A small molecule targeting the multifactorial nature of Alzheimer's dis-

ease. *Angewandte Chemie International Edition*, 2007, 46(20): 3689-3692.

[32] Li Y, Qiang X, Luo L, Yang X, Xiao G, Zheng Y, Cao Z, Sang Z, Su F Deng Y. Multitarget drug design strategy against Alzheimer's disease: Homoisoflavonoid Mannich base derivatives serve as acetylcholinesterase and monoamine oxidase B dual inhibitors with multifunctional properties. *Bioorganic & Medicinal Chemistry*, 2017, 25(2): 714-726.

[33] Sang, Z., Li, Y., Qiang, X., Xiao, G., Liu, Q., Tan, Z., Deng, Y. Multifunctional scutellarin–rivastigmine hybrids with cholinergic, antioxidant, biometal chelating and neuroprotective properties for the treatment of Alzheimer's disease. *Bioorganic & Medicinal Chemistry*, 2015, *23*(4): 668-680.

[34] Sang Z, Pan W, Wang K, Ma Q, Yu L, Yang Y, Bai P, Leng C, Xu Q, Li X, Tan Z, Liu W. Design, synthesis and evaluation of novel ferulic acid-O-alkylamine derivatives as potential multifunctional agents for the treatment of Alzheimer's disease. *European Journal of Medicinal Chemistry*. 2017, 130, 379-392.

[35] Di, L., Kerns, E. H., Fan, K., McConnell, O. J., Carter, G. T. High throughput artificial membrane permeability assay for blood–brain barrier. *European Journal of Medicinal Chemistry*, 2003, *38*(3): 223-232.

[36] Sang Z, Wang K, Han X, Cao M, Tan Z, Liu W. Design, synthesis, and evaluation of novel ferulic acid derivatives as multi-target-directed ligands for the treatment of Alzheimer's disease. *ACS Chemical Neuroscience*. 2019, *10*(2): 1008-1024.

[37] Sang, Z., Wang, K., Wang, H., Wang, H., Ma, Q., Han, X., Liu, W. Design, synthesis and biological evaluation of 2-acetyl-5-O-(amino-alkyl) phenol derivatives as multifunctional agents for the treatment of Alzheimer's disease. *Bioorganic & Medicinal Chemistry Letters*, 2017, *27*(22), 5046-5052.

[38] Pan, L. F., Wang, X. B., Xie, S. S., Li, S. Y., Kong, L. Y. Multitarget-directed resveratrol derivatives: anti-cholinesterases, anti-β-amyloid aggregation and monoamine oxidase inhibition properties against Alzheimer's disease. *MedChemComm*, 2014, *5*(5): 609-616.

[39] Li, Y., Qiang, X., Luo, L., Yang, X., Xiao, G., Liu, Q., Deng, Y. Aurone Mannich base deriv-

atives as promising multifunctional agents with acetylcholinesterase inhibition, anti-β-amyloid aggragation and neuroprotective properties for the treatment of Alzheimer's disease. *European Journal of Medicinal Chemistry*, 2017, *126*, 762-775.

[40] Huang, L., Lu, C., Sun, Y., Mao, F., Luo, Z., Su, T., Li, X. Multitarget-directed benzylidene-indanone derivatives: anti-β-amyloid (Aβ) aggregation, antioxidant, metal chelation, and monoamine oxidase B (MAO-B) inhibition properties against Alzheimer's disease. *Journal of Medicinal Chemistry*, 2012, *55*(19), 8483-8492.

[41] Mohamed, T., Rao, P. P. 2, 4-Disubstituted quinazolines as amyloid-β aggregation inhibitors with dual cholinesterase inhibition and antioxidant properties: Development and structure-activity relationship (SAR) studies. *European Journal of Medicinal Chemistry*, 2017, *126*, 823-843.

[42] Xu, P., Zhang, M., Sheng, R., Ma, Y. Synthesis and biological evaluation of deferiprone-resveratrol hybrids as antioxidants, Aβ1–42 aggregation inhibitors and metal-chelating agents for Alzheimer's disease. *European Journal of Medicinal Chemistry*, 2017, *127*, 174-186.

[43] Jiang, N., Li, S. Y., Xie, S. S., Li, Z. R., Wang, K. D., Wang, X. B., Kong, L. Y. Design, synthesis and evaluation of multifunctional salphen derivatives for the treatment of Alzheimer's disease. *European Journal of Medicinal Chemistry*, 2014, *87*, 540-551.

Figures, Schemes and Tables
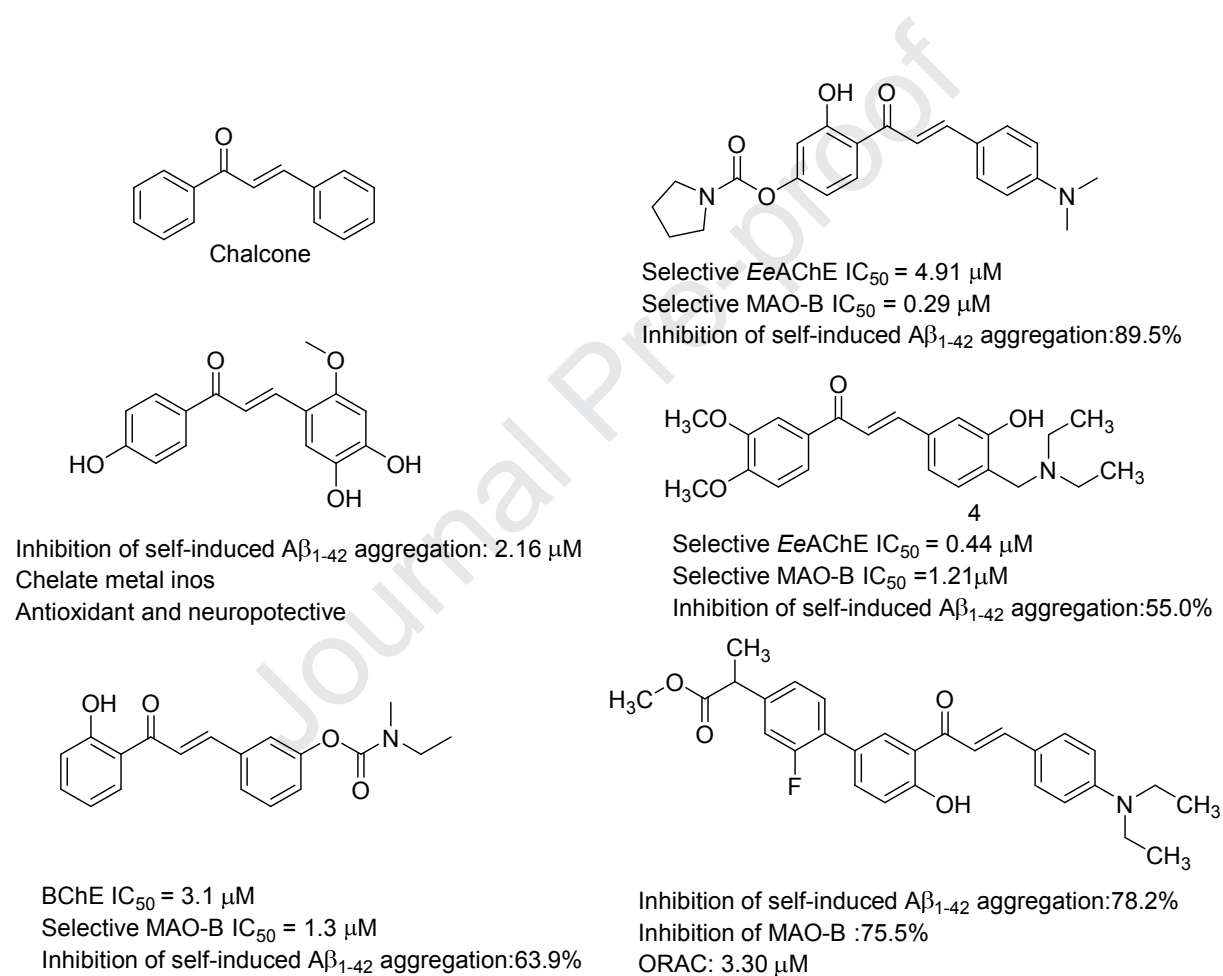
Fig. 1. Structure of chalcone skeleton and representative published multi-functional chalcone derivatives for AD treatment.
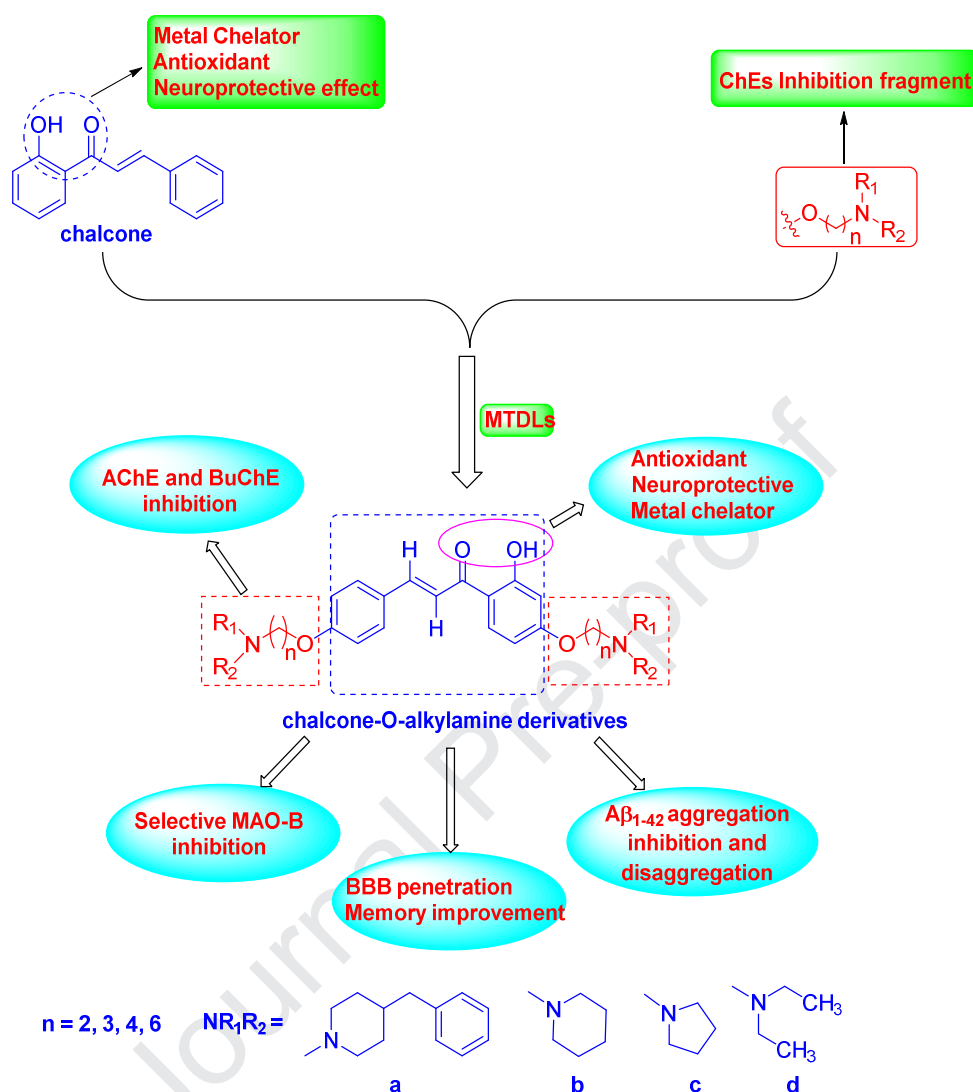
Fig. 2 Design strategy for the chalcone-*O*-alkylamine derivatives
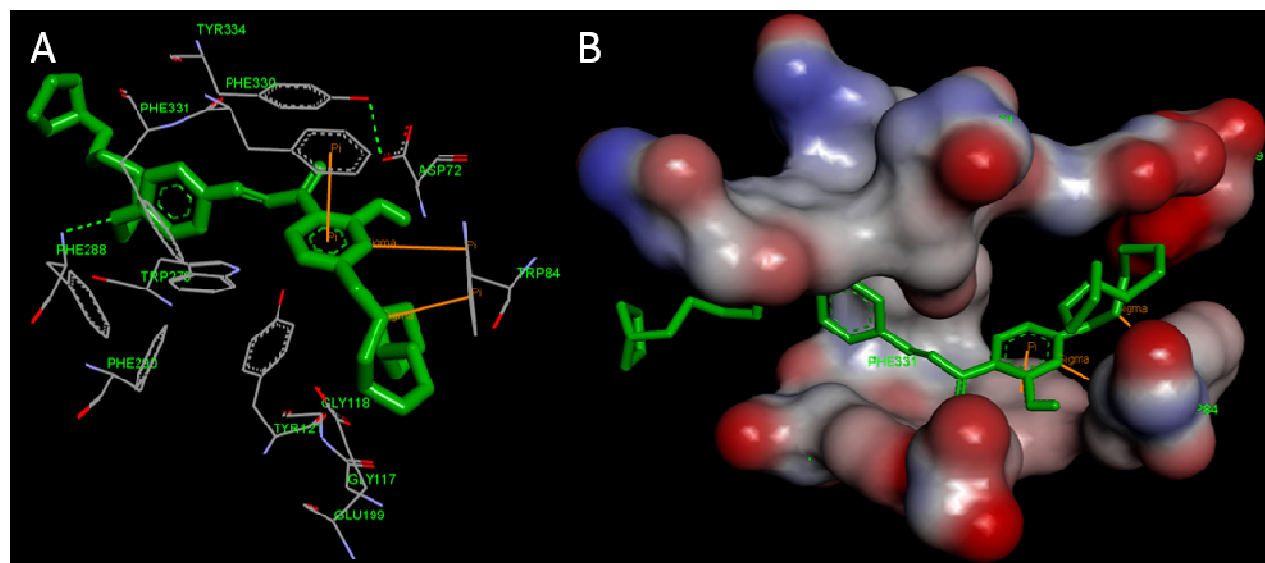
Fig. 3 (A) Representation of compound **23c** (green stick) interacting with residues in the binding site of *Tc*AChE (PDB code: 1EVE). (B) 3D docking model of compound **23c** with *Tc*AChE.
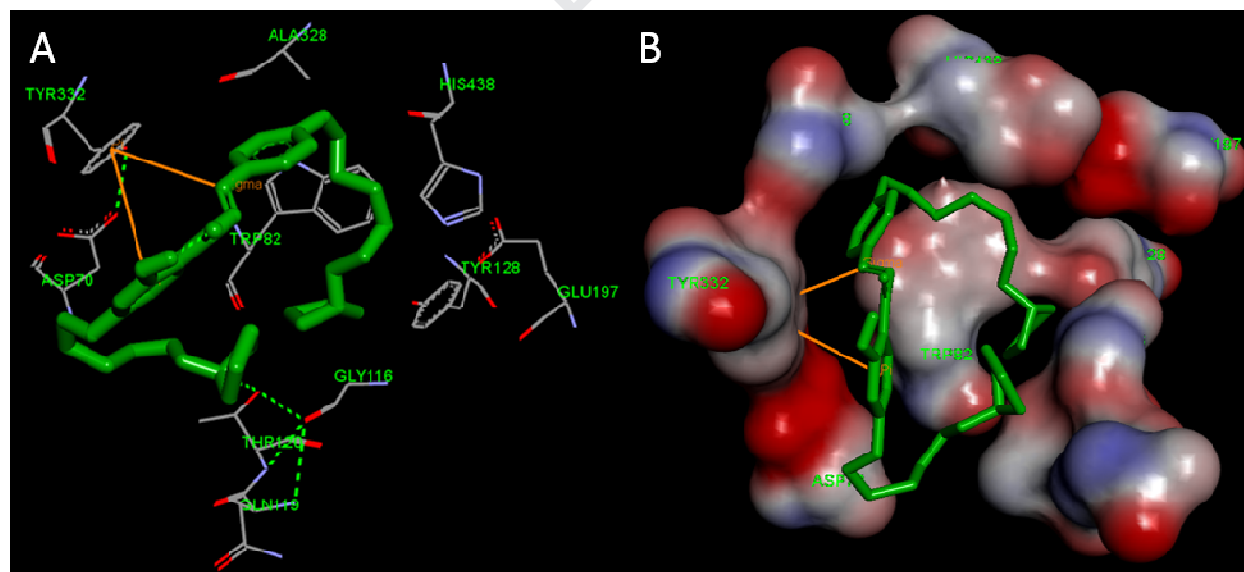
Fig. 4 (A) Representation of compound **23c** (green stick) interacting with residues in the binding site of *hu*BuChE (PDB code: 4tpk). (B) 3D docking model of compound **23c** with *hu*BuChE.
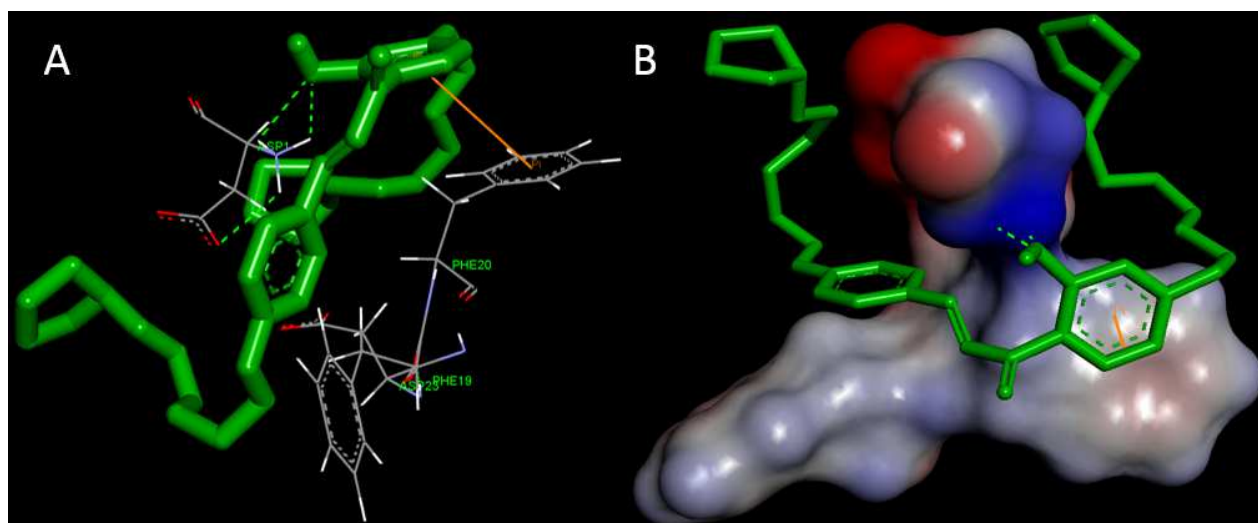
Fig. 5 (A) Representation of compound **23c** (green stick) interacting with residues in the binding site of A$\beta_{1\text{-}42}$ (PDB ID: 1BA4), highlighting the protein residues that participate in the main interactions with the inhibitor. (B) 3D docking model of compound **23c** (green stick) with Aβ.
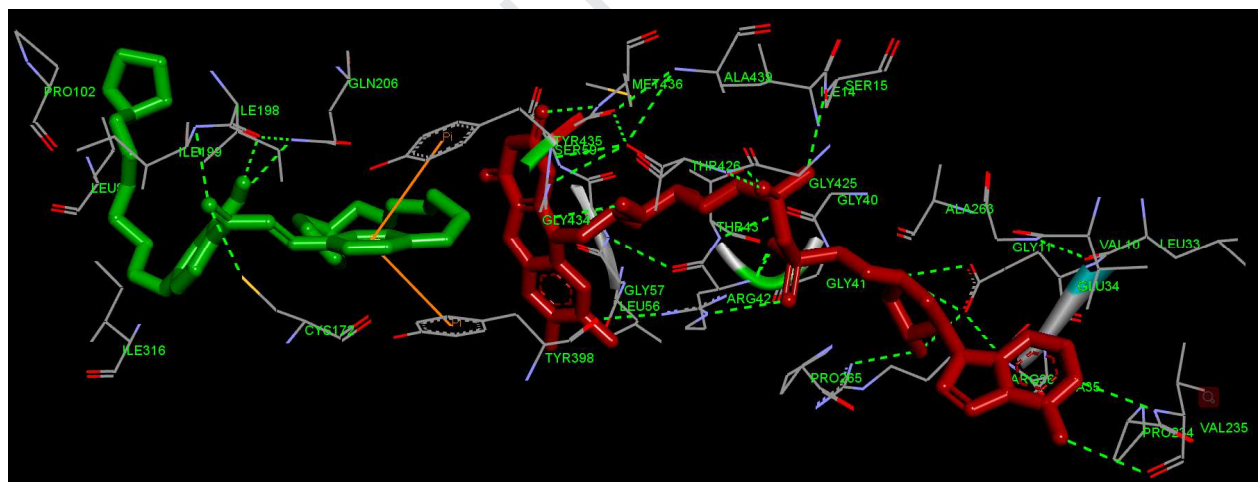
Fig. 6 Compound **23c** (green stick) interacting with residues in the binding site of MAO-B (PDB code: 2V60), highlighting the protein residues that participate in the main interactions with the inhibitor.
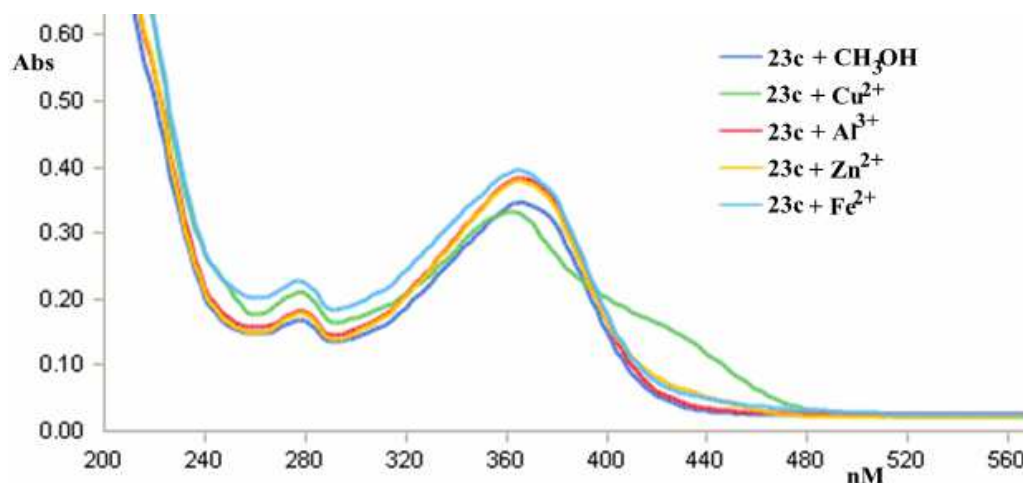
Fig. 7 The UV spectrum of compounds **23c** (37.5 μM, in methanol) alone or in the presence of CuCl$_2$, AlCl$_3$, ZnCl$_2$ and FeSO$_4$ (37.5 μM, in methanol)
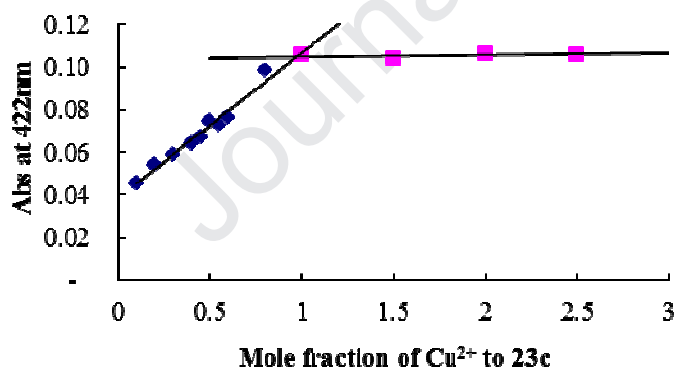
Fig. 8 Determination of the stoichiometry of complex-Cu^{2+} by using molar ratio method through titrating the methanol solution of compound **23c** with ascending amounts of CuCl$_2$. The final concentration of tested compound was 37.5 μM.

Inhibition experiment

A

$$A\beta \text{ (fresh)} + Cu^{2+} \xrightarrow[\text{2min, rt}]{} \xrightarrow[\text{24h, 37°C}]{\text{Chelator}} A\beta \text{ Species}$$
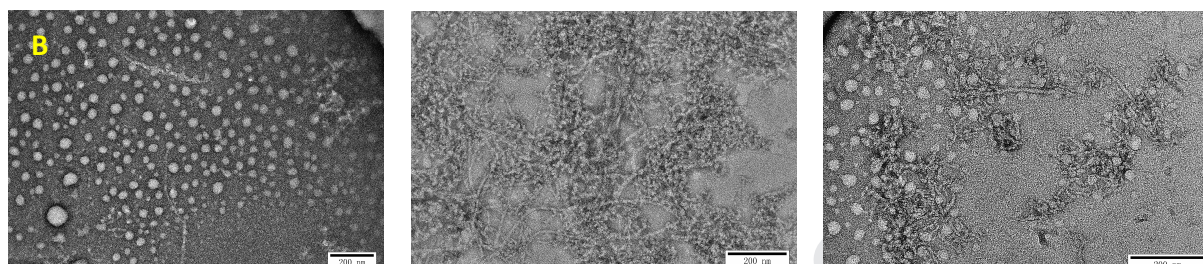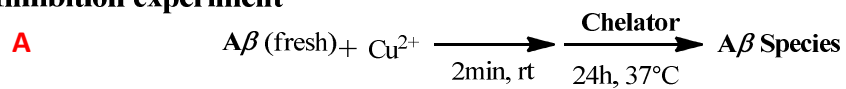
Aβ (0h)   Aβ + Cu^{2+} (24h)   Aβ + Cu^{2+} + **23c** (24h)

Disaggregation experiment

C

$$A\beta \text{ (fresh)} + Cu^{2+} \xrightarrow[\text{24h, 37°C}]{} A\beta \text{ Fibrils} \xrightarrow[\text{24h, 37°C}]{\text{Chelator}} A\beta \text{ Species}$$
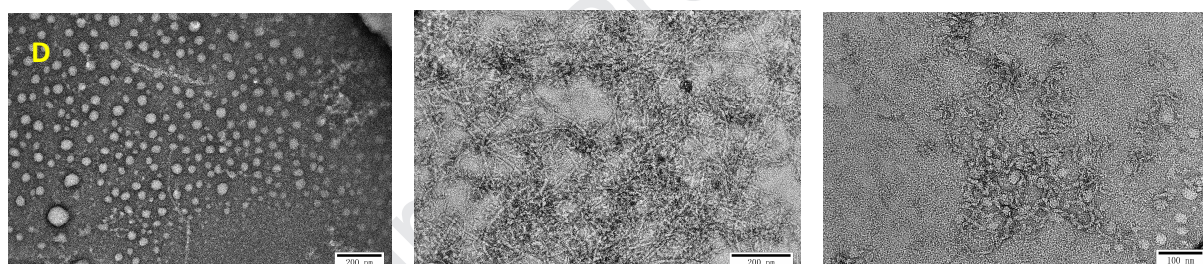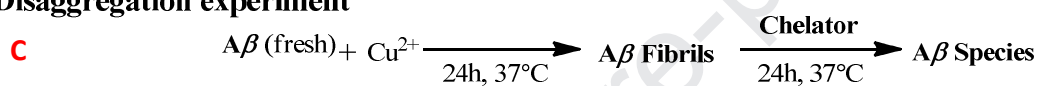
Aβ (0h)   Aβ + Cu^{2+} (48h)   Aβ + Cu^{2+} + **23c** (48h)

Fig. 9 (A) Scheme of the inhibition experiment; (B) TEM images of Aβ species from inhibition experiments. (C) Scheme of the disaggregation experiments; (D) TEM images of samples from disaggregation experiments.
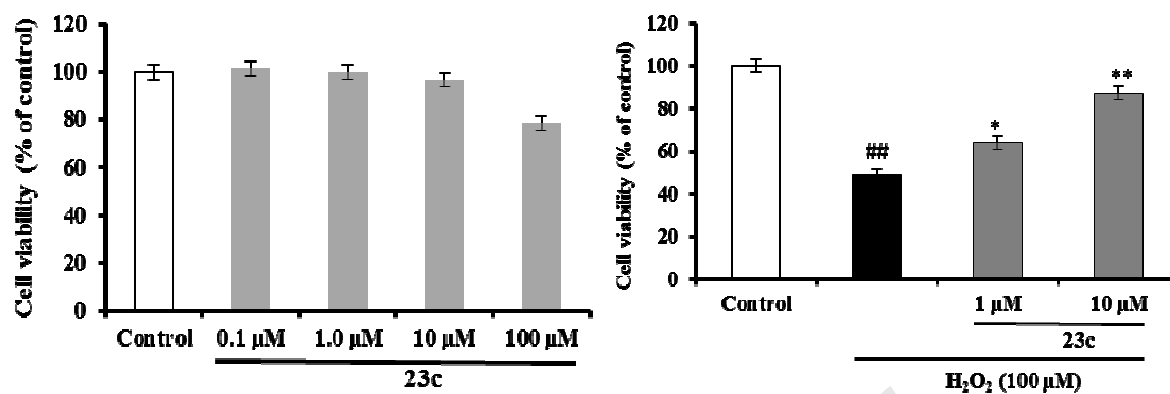
Fig. 10 (A) Effects of **23c** on cell viability in PC12 cells. (B) Protective effects of **23c** on cell injury induced by H_2O_2 (100 μM) in PC12 cells. $^{\#\#}P < 0.01$ *vs* control; $^{*}P < 0.05$ *vs* H_2O_2 group and $^{**}P < 0.01$ *vs* H_2O_2 group.
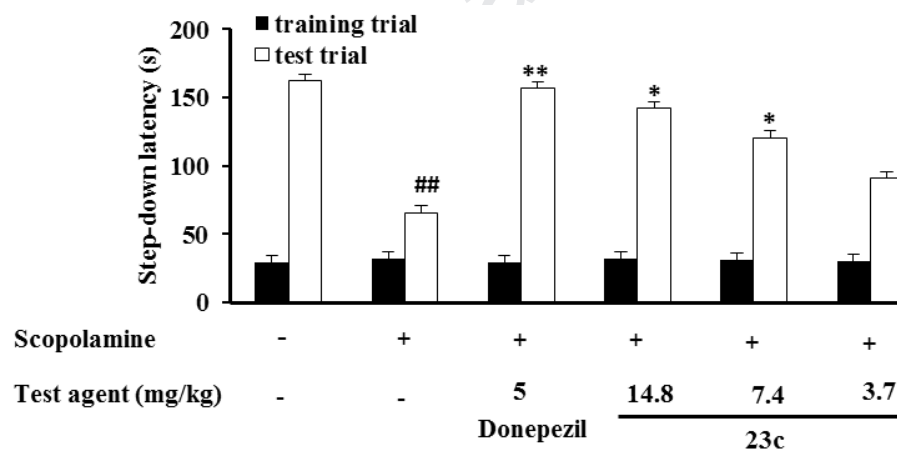
Fig. 11 Effects of compound **23c** on scopolamine-induced memory deficit in the step-down passive avoidance test. Values are expressed as the mean ± SEM (n=10). ## $p < 0.01$ *vs* normal group. * $p < 0.05$ and ** $p < 0.01$ *vs* model group (n = 10).
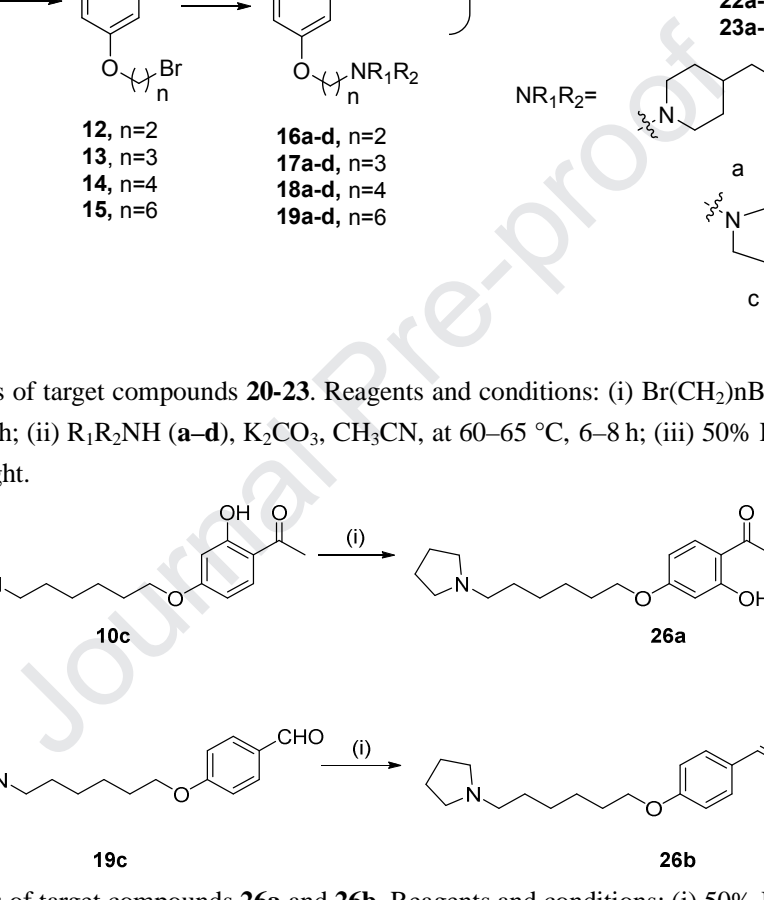
Scheme 1. Synthesis of target compounds **20-23**. Reagents and conditions: (i) Br(CH$_2$)nBr (**2a–2d**), K$_2$CO$_3$, acetone, reflux, 6–8 h; (ii) R$_1$R$_2$NH (**a–d**), K$_2$CO$_3$, CH$_3$CN, at 60–65 °C, 6–8 h; (iii) 50% KOH, EtOH, room temperature, overnight.
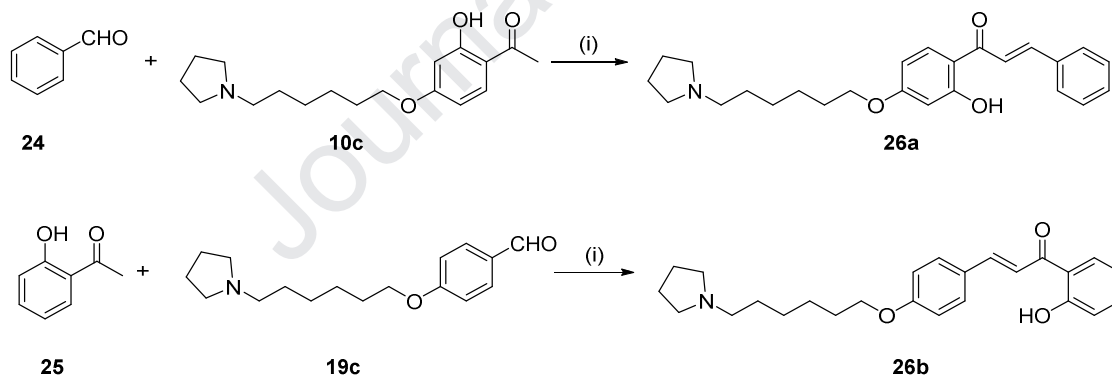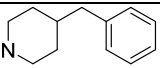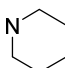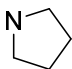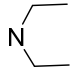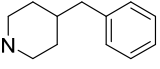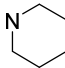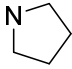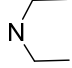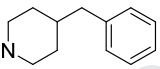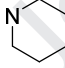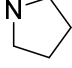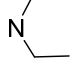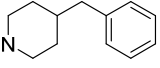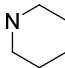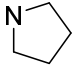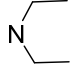

Scheme 2. Synthesis of target compounds **26a** and **26b**. Reagents and conditions: (i) 50% KOH, EtOH, room temperature, overnight.

Table 1 Inhibition of AChE/BuChE and MAO-B/MAO-A, and selectivities index of target compounds and reference compounds.

Table 2 Inhibition of *hu*AChE and *hu*BuChE for compound **23d** and reference compound donepezil.

Table 3 The antioxidant activity, and effect on A$\beta_{1\text{-}42}$ aggregation of chalcone-*O*-alkylamines derivatives and reference compounds.

Table 1. Inhibitions of AChE/BuChE and MAO-B/MAO-A of target compounds and reference compounds.

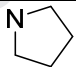| Compd.	n	NR$_1$R$_2$	IC$_{50}$ (μM) ± SD [a]		SI [d]	IC$_{50}$ (μM) ± SD [a]		SI [g]
			*ee*AChE [b]	*eq*BuChE [c]		MAO-B [e]	MAO-A [J]	
20a	2		23.9 ± 0.9	10.6 ± 0.1% [h]	---	21.6 ± 0.6	n.a. [j]	---
20b	2		19.6 ± 0.4	26.2 ± 0.2% [h]	---	17.2 ± 0.3	n.a. [j]	---
20c	2		1.80 ± 0.03	6.80 ± 0.15	3.8	8.10 ± 0.11	n.a. [j]	---
20d	2		3.10 ± 0.02	5.20 ± 0.04	1.7	9.70 ± 0.06	n.a. [j]	---
21a	3		21.8 ± 0.5	12.1 ± 0.1% [h]	---	16.8 ± 0.31	26.1 ± 0.87	1.6
21b	3		5.70 ±0.06	4.10 ±0.01	0.7	2.10 ± 0.45	10.1 ± 0.1% [i]	---
21c	3		0.79 ±0.01	3.80 ±0.19	4.8	8.30 ± 0.05	n.a. [j]	---
21d	3		4.70 ±0.05	5.90 ±0.22	1.3	1.50 ± 0.02	6.50 ± 0.02% [i]	---
22a	4		12.7 ±0.6	14.3 ± 0.9% [h]	---	15.4 ± 0.2	10.6 ± 0.3% [i]	---
22b	4		1.80 ±0.16	3.60 ± 0.27	2	0.87 ± 0.01	n.a. [j]	---
22c	4		3.16 ±0.02	4.50 ± 0.09	1.4	0.73 ± 0.02	n.a. [j]	---
22d	4		2.70 ±0.03	18.5 ± 0.9	6.9	0.66 ± 0.03	10.5 ± 0.4	19
23a	6		1.30 ±0.02	0.80 ±0.01	0.6	1.10 ± 0.16	12.5 ± 0.19% [i]	---
23b	6		1.86 ±0.31	3.50 ± 0.09	1.9	3.40 ± 0.12	n.a. [j]	---
23c	6		1.30 ±0.01	1.20 ± 0.09	0.9	0.57 ± 0.01	n.a. [j]	---
23d	6		3.70 ±0.04	4.20 ±0.26	1.1	1.60 ± 0.04	8.70 ± 0.05% [i]	---
26a			4.20 ±0.02	12.3 ±0.79	2.9	12.7 ± 0.26	9.5 ± 0.02% [i]	---

26b	8.90 ±0.05	50.2 ±0.62	5.6	18.5 ± 0.51	15.6 ± 0.08%[i]	---
Ipro[l]	n.t.[o]	n.t.[o]		1.35 ± 0.02	5.48 ± 0.03	4.1
Rasa.[m]	n.t.[o]	n.t.[o]		0.0281±0.0068	0.587 ± 0.038	20.9
Done.[n]	0.019±0.0003	4.76±0.02	251	n.t.[o]	n.t.[o]	

[a] IC_{50} values represent the concentration of inhibitor required to decrease enzyme activity by 50% and are the mean of three independent experiments, each performed in triplicate (SD = standard deviation). [b] From *electrophorus electricus*. [c] *Eq*BuChE from *equine serum*. [d] SI = selectivity index = IC_{50} (BuChE)/IC_{50} (AChE). [e] From recombinant human MAO-B. [f] From recombinant human MAO-A. [g] hMAO-B selectivity index = IC_{50} (MAO-A)/IC_{50} (MAO-B). [h] The *eq*BuChE inhibition percentage of compounds at 25 μM. [i] The MAO-A inhibition percentage of compounds at 10 μM. [j] n.a. = no active, representing MAO-A inhibition percentage of compounds < 5% at 10 μM. [l] Ipro. = Iproniazid. [m] Rasa. = Rasagiline. [n] Done. = Donepezil. [o] n.t. = not tested.

Table 2 Inhibition of *hu*AChE and *hu*BuChE for compound **23d** and reference compound donepezil.

Compound	n	NR_1R_2	IC_{50} (μM) ± SD [a]		SI [d]
			*hu*AChE [b]	*hu*BuChE [c]	
23c	6	N⟨	0.78 ±0.02	0.91 ± 0.03	1.2
26a			3.2 ±0.01	15.8 ±0.49	
Donepezil			0.011±0.0008	5.12±0.06	465

[a] IC_{50} values represent the concentration of inhibitor required to decrease enzyme activity by 50% and are the mean of three independent experiments, each performed in triplicate (SD = standard deviation). [b] From *human* AChE. [c] From *human* BuChE. [d] SI = selectivity index = IC_{50} (BuChE)/IC_{50} (AChE).

Table 3 Antioxidant activity, and effect on Aβ_{1-42} aggregation of chalcone-*O*-alkylamines derivatives and reference compounds.

Compound	ORAC [a]	Effect on of Aβ_{1-42} aggregation (%)[b]		
		Inhibit self-induced [c]	Inhibit Cu^{2+}-induced [d]	Disaggregate Cu^{2+}-induced [e]
20a	1.0 ± 0.01	53.5 ± 0.5	n.t. [f]	n.t. [f]
20b	1.2 ± 0.01	59.8 ± 0.3	n.t. [f]	n.t. [f]
20c	1.1 ± 0.01	61.3 ± 0.6	86.1 ± 0.5	n.t. [f]
20d	0.96 ± 0.01	63.1 ± 0.5	85.2 ± 0.7	n.t. [f]
21a	0.99 ± 0.01	61.8 ± 0.8	n.t. [f]	n.t. [f]
21b	1.20 ± 0.20	65.7 ± 0.8	74.1 ± 0.6	n.t. [f]
21c	0.99 ± 0.02	60.9 ± 0.86	80.2 ± 0.7	n.t. [f]
21d	0.98 ± 0.01	64.7 ± 0.8	75.9 ± 0.6	n.t. [f]
22a	1.20 ± 0.01	62.7 ± 0.5	n.t. [f]	n.t. [f]
22b	1.10 ± 0.02	71.8 ± 0.7	83.6 ± 0.7	n.t. [f]
22c	0.97 ± 0.02	63.1 ± 0.6	84.5 ± 0.8	n.t. [f]
22d	1.20 ± 0.01	62.7 ± 0.7	n.t. [f]	n.t. [f]
23a	1.10 ± 0.01	51.3 ± 0.3	n.t. [f]	n.t. [f]
23b	1.40 ± 0.02	61.8 ± 0.4	86.5 ± 0.6	n.t. [f]
23c	1.30 ± 0.01	68.3 ± 0.6	81.2 ± 0.6	70.4 ± 0.5
23d	1.10 ± 0.01	63.7 ± 0.6	84.2 ± 0.5	n.t. [f]
Curcumin	n.t. [f]	47.3 ± 0.01	76.5 ± 0.02	56.5 ± 0.2
Donepezil	n.t. [f]	n.a. [g]	n.t. [f]	n.t. [f]

[a] Results were expressed as μM of Trolox equivalent/μM of tested compounds. [b] Inhibition of Aβ_{1-42} aggregation and disaggregation of Aβ_{1-42} aggregates, the thioflavin-T fluorescence-based method was used, data are the mean $\pm$ SEM of three independent experiments. [c] Inhibition of self-Induced Aβ_{1-42} aggregation, the concentration of tested compounds and Aβ_{1-42} were 25 μM. [d] Inhibition of Cu^{2+}-induced Aβ_{1-42} aggregation. The concentration of tested compounds and Cu^{2+} both were 25 μM. [e] Disaggregating of Cu^{2+}-induced Aβ_{1-42} aggregates, the concentration of tested compounds and Aβ_{1-42} were 25 μM. [f] n.t. = not tested. [g] n.a. = no active. Compounds defined "not active" showed a % inhibition lower than 5.0% at 25μM.

Highlights

- A series of novel chalcone-*O*-alkylamine derivatives was design based on MTDLs strategy.

- Compound **23c** displayed the best inhibitory potency both on acetylcholinesterase ($IC_{50} = 1.3 \pm 0.01$ μM) and butyrylcholinesterase ($IC_{50} = 1.2 \pm 0.1$ μM).

- Compound **23c** exhibited the best selective MAO-B inhibitory activity

- Compound **23c** showed good antioxidant activity, and displayed significant neuroprotective activity against H_2O_2-induced PC12 cell injury.

- Compound **23c** exhibited significant inhibition and disaggregation effects on $A\beta_{1-42}$ aggregation.

- Compound **23c** could improve scopolamine-induced memory impairment.